Spring 2019

An in-situ Study of the Aqueous Speciation of Uranium (VI) Under Hydrothermal Conditions

Diwash Dhakal

Missouri State University, Dhakal86@live.missouristate.edu

Recommended Citation

AN *IN-SITU* STUDY OF THE AQUEOUS SPECIATION OF URANIUM (VI)

UNDER HYDROTHERMAL CONDITIONS

A Master's Thesis

Presented to

The Graduate College of

Missouri State University

In Partial Fulfillment

Of the Requirements for the Degree

Master of Science, Materials Science

By

Diwash Dhakal

May 2019

AN *IN-SITU* STUDY OF THE AQUEOUS SPECIATION OF URANIUM (VI) UNDER

HYDROTHERMAL CONDITIONS

Physics, Astronomy and Materials Science

Missouri State University, May 2019

Master of Science

Diwash Dhakal

ABSTRACT

Rigorous study of the speciation distribution of uranyl-chloride bearing solutions under hydrothermal conditions is important to understand the transport mechanism of uranium underground, which is of uttermost interest to parties studying the geological uranium deposits and those studying the possibilities of geological repositories for spent nuclear waste. I report an *in-situ* Raman spectroscopic study of the speciation distribution of aqueous uranyl-chloride complexes upto 500°C conducted using a HDAC as the high PT spectroscopic cell. The samples studied contained the species UO_2^{2+}, UO_2Cl^+, $UO_2Cl_2^0$ and $UO_2Cl_3^-$ with varying contributions at different temperature and chloride concentration conditions. Raman vibrational peak positions and the FWHM were determined for each of the identified species, and speciation distribution graphs were plotted for different temperature and concentration points. The results obtained are in good agreement with the published room temperature data and also with a high temperature study performed using UV-Vis spectroscopy technique. To confirm and complement the knowledge obtained from optical spectroscopy techniques like Raman spectroscopy and UV-Vis spectroscopy, x-ray absorption spectroscopy experiments are very useful, but the use of radioactive samples under high pressure and temperature conditions in synchrotron x-ray facilities requires strict protocols and a special radiological containment system. I designed and assembled a radiological enclosure system for HDAC suited for synchrotron x-ray absorption spectroscopy experiments on aqueous actinide samples upto high temperature and pressure. This enclosure was successfully tested at APS and SSRL after the approval from radiological safety committee of the respective facilities. XAS data were collected from the uranyl samples upto 500°C and were found to be of comparable quality to those from similar experiments on non-rad samples without the use of enclosure. One representative set of x-ray absorption spectra for aqueous uranyl-chloride bearing sample upto 500°C is presented in this thesis.

KEYWORDS: uranium speciation, hydrothermal diamond anvil cell, Raman spectroscopy, x-ray absorption spectroscopy, high pressure high temperature

AN *IN-SITU* STUDY OF THE AQUEOUS SPECIATION OF URANIUM (VI) UNDER

HYDROTHERMAL CONDITIONS

By

Diwash Dhakal

A Master's Thesis
Submitted to the Graduate College
Of Missouri State University
In Partial Fulfillment of the Requirements
For the Degree of Master of Science, Materials Science

May 2019

Approved:

Robert A. Mayanovic, Ph.D., Thesis Committee Chair

Kartik C. Ghosh, Ph.D., Committee Member

Tiglet Besara, Ph.D., Committee Member

Julie Masterson, Ph.D., Dean of the Graduate College

In the interest of academic freedom and the principle of free speech, approval of this thesis indicates the format is acceptable and meets the academic criteria for the discipline as determined by the faculty that constitute the thesis committee. The content and views expressed in this thesis are those of the student-scholar and are not endorsed by Missouri State University, its Graduate College, or its employees.

ACKNOWLEDGEMENTS

In dedication to my beloved dad Prof. Kishor P. Dhakal and mom Nirmala Dhakal.

TABLE OF CONTENTS

LIST OF TABLES

LIST OF FIGURES

OVERVIEW

Uranium is an *f*-block element, with atomic number 92 and symbol 'U', in the actinide series of the periodic table. It is a silver-grey colored metal at RTP, with a high density of about 19.1 gm/cm^3, comparable to that of gold and titanium. It has 92 protons, 92 electrons and varying number of neutrons, depending on the isotope. For instance, ^{238}U has 146 neutrons while ^{235}U has 143 neutrons. The most common naturally occurring isotope is the ^{238}U (>99%) and the second ^{235}U (<0.8%). All the isotopes of uranium are unstable and hence radioactive, with varying half-lives; few hundred million years (^{235}U) and few billion years (^{238}U). Uranium (^{235}U) decays by emitting an alpha particle, which is a system of 2 protons and 2 neutrons, equivalent to a He-4 nucleus. Most of the naturally occurring uranium is found in compound form in various minerals.

Uranium exists in multiple valency states: U(VI), U(V), U(IV), U(III), U(II), and U(I); the most stable and the most mobile state of which is the hexavalent state U (VI). In aqueous solution it readily bonds covalently with two oxygens in a linear structural symmetry (O=U=O, angle=180°) to form the uranyl ion (UO_2^{2+}). The chemistry of the uranyl ion in aqueous solution, more importantly in the hydrothermal state, is very complex and of critical value. The uranyl ion can easily form complexes with different ligands such as sulphate, carbonate, chloride, etc., more readily in hydrothermal conditions and may play an important role in the transport of uranium in aqueous systems. Fig. 1.1 shows the structure of a representative complex formed by the uranyl ion with addition of 3 water molecules (only oxygen atoms are shown (red)) and 2 chloride ions.
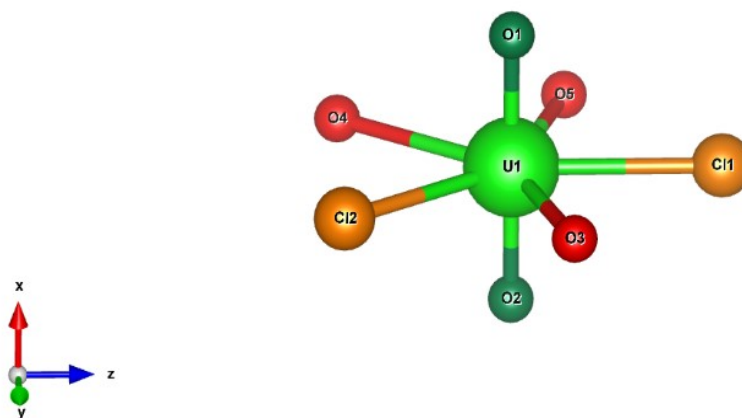
Fig. 1.1: Schematic showing the structure of $UO_2(OH_2)_3Cl_2^0$ complex. Oxygen atoms in red are the ones from water molecules.

Despite the importance, studies on aqueous properties of uranyl ions at elevated temperatures and pressures are scarce and the knowledge is not comprehensive [1].

In-situ studies of speciation of uranium under hydrothermal conditions is necessary to address a variety of pressing issues of interest in the nuclear energy sector, including the viability of geological repositories for spent nuclear fuels [2]–[5], accidental meltdowns such as the Fukushima disaster, and the development of accident-tolerant nuclear fuels [6], [7]. Study have shown that the temperature in deep geological repositories of spent nuclear fuels can reach up to 200°C due to radioactivity [8]. The knowledge of the transport mechanisms of uranium in hydrothermal environment will aid in the minimum-risk-design and positioning of the proposed geological nuclear waste repositories and in understanding, assessing and mitigating the risks associated with nuclear accidents. Thus, the knowledge of speciation and successive transport mechanism of uranium at elevated temperature plays a vital role in aiding the implementation of geological repositories for spent nuclear fuels.

This is also a subject of interest for geologists to understand the processes involved in the formation of geological uranium deposits [1], [9], [10], which is mostly influenced by the effective dissolution, transport and deposition of uranium in aqueous hydrothermal conditions, which in turn is highly corelated with the uranyl complex formation and the kind and amount of different species (i.e. speciation) formed in that given condition. The knowledge of speciation of uranium in hydrothermal aqueous environment is pivotal to the understanding of the behavior and the fate of uranium in geo-fluids leading to ore formation [1]. Scientists [11], [12] have shown that a considerable portion of uranium in the world was deposited through hydrothermal scavenging, transport and deposition process, including some huge deposits like the McArthur River uranium deposit in Canada and the Olympic Dam deposit in Australia. This certainly points towards an urgent need for the better understanding of the key mechanisms governing dissolution, transport and deposition of uranium especially at elevated temperatures and pressures to understand, model and predict the conditions and processes involved during uranium ore formation.

Chloride is one of the most common and readily available ligands in naturally occurring hydrothermal systems. This includes hydrothermal fluids at proposed geological repository sites and ones responsible for the formation of ores over geological spans of time. Chloride is also a crucial complexing ligand that may be involved in the transport of uranium during nuclear accidents like Fukushima disaster, relating to the saline water of the oceans. Studies of natural samples collected from giant deposit sites including the Olympic Dam deposit in Australia and McArthur River deposit in Canada have shown chloride concentrations exceeding 40wt% NaCl equivalent [11], [13], [14]. This is supported by separate studies made on fluid inclusions collected from other uranium deposits formed under hydrothermal conditions, which also show

high chloride concentrations [15]–[17]. Despite the conjecture that aqueous uranyl chlorides are weak complexes [18] at ambient conditions (i.e. the UO_2^{2+} – Cl^- bond is purportedly relatively weak), higher chloride concentration and elevated temperature conditions of the sample solutions can potentially favor in overcoming this weakness and compete well with other potential ligands to make uranyl chloride complex more important in the transport of uranium in chloride rich aqueous systems [9]. This trend can become even more pronounced at even more extreme temperatures and eventually chloride can become a dominant complexing ligand in hydrothermal conditions, thus controlling the uranium distribution and transport mechanism. This has been shown to be the case for rare earth elements, which are often thought of as analogs for the actinides [19]. Here, it was shown that the weak chloride complexes can compete successfully with other species at high chloride concentrations, typical of ore forming geo-fluids. These findings suggest that uranyl-chloride complexation is important in the transport and ultimate fate of uranium under hydrothermal conditions.

The studies outlined above suggest the importance of uranyl chloride complexation in the transport and ultimate fate of uranium under hydrothermal conditions. In addition, these studies show promise for achieving a better understanding of processes involved in the formation of natural uranium deposits and for aiding in the design and selection of geological nuclear waste repositories for the future.

The importance of the study of aqueous uranyl-chloride complexation and determination of the species formed under hydrothermal conditions is paramount: however, studies on this are scarce. On the contrary, most of the data available on this system are for ambient pressure-temperature (PT) conditions only. Studies of aqueous uranyl-chloride solutions have been made employing different experimental characterization approaches such as spectroscopy, X-ray

scattering, chromatography and electromotive force measurements, all made under ambient conditions [20]–[23]. These studies identified the uranyl species in terms of the co-existence of multiple species, UO_2^{2+}, UO_2Cl^+, $UO_2Cl_2^0$ and $UO_2Cl_3^-$ in aqueous solutions at ambient temperature. A separate study which investigated the structure of uranyl-chloride complexes in the aqueous environment at room temperature employing EXAFS, identified the aqueous species as UO_2^{2+}, UO_2Cl^+ and $UO_2Cl_2^0$ [24]. However, studies covering the high temperature regime of this aqueous uranyl-chloride complex system are limited to those made by Dargent *et al.* [10] and Migdisov *et al.* [9]. Interestingly, these two independent studies employing separate spectroscopic techniques (Raman for the former and UV-Vis for the latter study) ended up with very different speciation results under similar PT conditions for aqueous solutions having similar uranyl/chloride concentrations. Dargent *et al.* [10] employed high temperature in-situ Raman spectroscopy to study the speciation of aqueous uranyl-chloride complex in acidic solutions up to 350°C. They identified species that consisted of $UO_2Cl_4^{2-}$, $UO_2Cl_5^{3-}$ and one additional unnamed specie in addition to the ones found at room temperature by other groups [20]-[23]. Moreover, they show that at higher temperature and chloride concentration the species distribution of the aqueous uranyl-chloride complex is dominated by these four-chloro and five-chloro species and one other species that they were not able to identify. This finding of the occurrence of highly charged species at higher temperatures contrasts with the general understanding of hydrothermal solutions. In such solutions, generally, increase in temperature destabilizes highly charged species and favors the formation of neutral and less charged species owing to the changing properties of water, especially the strong reduction of the dielectric constant [9], [19]. When the dielectric constant of water reduces with increase in temperature, the shielding of highly charged species provided by water molecules becomes less effective, which effectively favors the

stabilization of neutral and less charged species at elevated temperatures. Migdisov *et al.* [9] studied the uranyl-chloride complexation in aqueous solutions up to 250°C using UV-Vis spectroscopic techniques. In contrast with the results from Dargent *et al.* [10], Migdisov *et al.* [9] proposed a speciation distribution that does not incorporate the highly charged species $UO_2Cl_4^{2-}$ and $UO_2Cl_5^{3-}$ at elevated temperatures (up to 250°C) and explained the discrepancy for the results from former group using an inappropriate theoretical model. Clearly, further experiments are required to resolve the conflicting results obtained by these two groups. This is necessary in order to establish the speciation behavior of aqueous uranyl-chloride under hydrothermal conditions. The motivation for the study presented in this thesis arose from the need for a careful investigation of the speciation distribution of uranyl-chloride complex at elevated temperatures and pressures in acidic solutions.

In this study, I used Raman spectroscopy and synchrotron x-ray absorption spectroscopy to investigate the structure of uranyl-chloride complexes and to identify different uranyl species in aqueous solutions under elevated PT conditions. These measurements were performed using the hydrothermal diamond anvil cell (HDAC) as the containment vessel for the aqueous samples. The full analysis of the x-ray absorption data for such hydrothermal system needs theoretical support and is beyond the scope of this thesis. Some of the preprocessed data are presented in Chapter 2. The focus of this thesis for the XAS part will be to introduce the design of a radiological enclosure for the HDAC and to demonstrate its implementation at synchrotron beamlines.

Performing an in-situ high pressure high temperature experiment on aqueous samples containing radioactive materials requires a great deal of preparatory work to be made on the laboratory, particularly for XAS measurements made at synchrotron facilities housed in national

laboratories. For this, a versatile spectroscopic cell is required that is capable of producing high pressure and temperature while enabling monitoring of the sample using various characterization probes. In addition, this cell also needs to be small and portable enough to be contained in a suitable radiological containment system in order to be used at synchrotron facilities. The HDAC meets all these requirements and has been used for similar experiments on non-rad samples [25] successfully without having the enclosure requirements. The HDAC can be used to produce the pressures and temperatures used for my experiment with very good precision (>98%), while providing accessibility for the incoming and outgoing beams (laser or x-ray) for characterization and is small enough to be contained using a specially designed radiological containment system.

Raman spectroscopy is a very useful tool when it comes to the study of the properties of molecules and their local coordination. This technique is equally effective for all the phases of matter; gas, liquid and solid, that have active Raman modes. A Raman mode of a molecule is active if it is allowed by the rules of Quantum Mechanics. This technique primarily relies on the Raman scattering of photons by the molecule in question. When suitable light photons, having wavelengths in the visible region, are scattered by molecules, most of the photons are scattered elastically, without any loss of energy. This is called Rayleigh scattering. A tiny fraction of the photons also gets scattered inelastically via the Raman process: The inelastic scattering results either in a loss or gain of energy, called Stokes or Anti-Stokes scattering respectively. The inelastic scattering is related to the excitation and relaxation of molecules in their vibrational states and, in addition, occasionally rotational states in case of gas molecules. Fig. 1.2 shows the general idea of the mechanism of Raman scattering. Upon absorption of the incident photon of light, the molecule or ion complex of the system is first excited from a particular vibrational state to a virtual state. The subsequent relaxation of the system occurs to either a higher vibrational
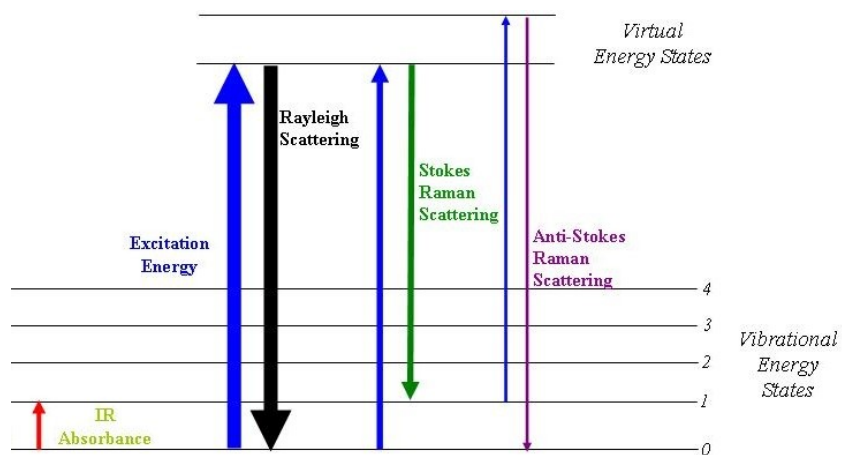
Fig. 1.2: Showing the general schematics of the Quantum mechanical interpretation of elastic and inelastic photon scattering by a molecule *(source: www.commons.wikimedia.org)*

state (Stokes scattering) or to a lower vibrational state (Anti-Stokes scattering). Either relaxation is accompanied by emission of a photon corresponding to the energy difference between the virtual and final vibrational states. The evolution of any molecule or a complex ion in an aqueous medium resulting from the change in its local environment is generally manifested by a change in the features of the Raman band of the original molecule or ion. In this thesis, I present an *in-situ* study of the change in features of the uranyl symmetric stretching vibrational band originally centered at about 870 cm^{-1}. The changing features of the band are related to the changing contribution of various species formed at different temperature, pressure and concentration conditions of the sample.

X-ray absorption spectroscopy is another technique that can furnish information about the local structure environment, i.e. the local geometry and coordination number of the ligands or neighboring atoms/ions that bond to the target atom (or ion) being probed. It can also be used to verify the speciation results obtained from Raman spectroscopy. In particular, the XAS can be used to gain information about the local coordination of an element. The XAS process involve the quantum mechanical scattering of the photo-electrons by neighboring atoms or ligands, upon

the absorption of X-rays in the immediate vicinity of the target atom; in this case, the target atom is U. XAS typically requires a high energy tunable X-ray source which is only available in state-of-the-art synchrotron facilities. As alluded to above, the selection of radioactive samples for XAS studies at synchrotron facilities demands full containment of such samples at all times during the experiments. The Department of Energy (DOE) synchrotron facilities stipulate the use of three independent layers of radiological containment for the samples containing radioactive materials. Because an aqueous radioactive material has never been studied before at high pressures and temperatures in an HDAC, a significant portion of the work for my thesis project required developing an enclosure system for the HDAC that fulfills the DOE containment requirements. I designed, tested and demonstrated the successful use of a radiological containment system especially suited for the containment of an HDAC for studying radioactive aqueous sample at high PT conditions at synchrotron beamlines. This containment system was approved and tested in XAS beamlines at the Advanced Photon Source (APS) and at the Stanford Synchrotron Radiation Lightsource (SSRL). The detailed structure and functions of the HDAC and the design and functioning of the radiological containment system are described in Chapter 2.

CHAPTER 1: AN *IN-SITU* RAMAN SPECTROSCOPIC STUDY OF URANYL CHLORIDE COMPLEXATION IN AQUEOUS ACIDIC SOLUTIONS UNDER HYDROTHERMAL CONDITIONS

Abstract. An in-situ experiment was designed and executed to conduct a Raman spectroscopic study of the aqueous speciation of Uranyl ion (0.05 M) under hydrothermal conditions in solutions, with 0.2 to 3 M chloride concentration values, and up to 500°C temperature and 500 MPa pressure. By fitting the Raman spectra, I was able to identify the following species at temperatures ranging from 25 to 500°C: UO_2^{2+}, UO_2Cl^+, $UO_2Cl_2^0$ and $UO_2Cl_3^-$, depending upon the total chloride concentration in the aqueous solutions. The speciation distributions were determined as a function of temperature for the solutions of study, and as a function of chloride concentration, from the measured Raman spectra. My speciation results at room temperature generally agree with the published results for room temperature and helps to resolve the uranyl speciation at elevated pressure-temperature conditions. My study shows that chloride complexes are effective in the transport of uranium in low pH chloride-bearing hydrothermal fluids.

Introduction

Experimental *in-situ* studies of aqueous speciation of uranium, especially in hydrothermal environments, is a subject of great interest for geologists studying uranium deposits [1]–[3]. Scientists have shown that a considerable portion of uranium in the world was deposited through hydrothermal scavenging, transport and deposition process [4], [5], including some very large deposits including the McArthur River uranium deposit in Canada and the Olympic Dam deposit

in Australia. Formation of uranium ores is influenced by the effective dissolution, transport and deposition of uranium in aqueous hydrothermal conditions. Thus, the speciation and successive transport mechanism of uranium at elevated temperature and pressure (P-T) conditions plays a vital role in aiding the understanding, modelling and prediction related to these geological processes.

Chloride is a common and important ligand in naturally occurring hydrothermal systems, including the ones responsible for the formation of ores over long periods of time. Studies of the samples collected from some giant deposits, such as the Olympic Dam deposit in Australia and McArthur River deposit in Canada, have shown chloride concentrations in the excess of 40 wt% NaCl equivalent [4], [6], [7]. In addition, analyses of fluid inclusions in uranium-bearing rocks from a large group of uranium deposits formed under hydrothermal conditions show high chloride concentrations [8]–[10].

Whereas aqueous uranyl chlorides are considered weak complexes [11] at ambient conditions, higher chloride concentrations or elevated temperatures can potentially overcome this and compete effectively with other so-called stronger (i.e., greater probability of formation) ligands to make uranyl chloride complexes important in the transport of uranium in chloride rich aqueous systems [3].

Despite the importance of chloride-bearing hydrothermal fluids in the transport of uranium, this system has not been well studied. The majority of the studies made on uranium in chloride rich aqueous solutions have been carried out under ambient conditions [12]–[15]. These studies employed various techniques, such as Raman spectroscopy, x-ray scattering, x-ray absorption spectroscopy, chromatography and electromotive force measurements, and identified the co-existence of UO_2^{2+}, UO_2Cl^+, $UO_2Cl_2°$ and $UO_2Cl_3^-$ species at room temperature. Hennig *et*

al. [16] used EXAFS to identify UO_2^{2+}, UO_2Cl^+, $UO_2Cl_2°$ and $UO_2Cl_3^-$ species in aqueous solutions having 0 – 9 M Cl at room temperature. However, the studies extending to higher P-T conditions are limited to those of Dargent *et al.* [1], who used Raman spectroscopy, and Migdisov *et al.* [3], who used UV-Vis spectroscopy. These groups studied similar uranyl-bearing aqueous solutions having chloride concentration upto 1.5 m [3] and upto 12 M [1]. Interestingly, the two groups proposed contrasting speciation distributions of the aqueous uranyl chloride complexes at elevated temperatures. Dargent *et al.* [1] proposed a speciation distribution consisting of uranyl chloride species with higher charge, namely $UO_2Cl_4^{2-}$ and $UO_2Cl_5^{3-}$ in addition to the ones found by other groups at room temperature. Conversely, Migdisov *et al.* [3] did not find evidence for such highly charged species and concluded that the dominant contribution at higher temperature was from the neutral and less charged species, including $UO_2Cl_2°$ and UO_2Cl^+ or $UO_2Cl_3^-$. The results of the latter group are more consistent than those of the former group with the general tendency of metal ion complexes trending toward neutral species with increasing temperature, due to the substantial reduction of the dielectric constant of water, in hydrothermal solutions. Such contrasting and conflicting results obtained on the same system by these two groups present a challenge in developing an understanding of the uranyl-chloride hydrothermal system. This conflict needs to be resolved in order to further understand the speciation behavior of uranium in hydrothermal fluids for a range of chloride concentrations. The purpose of my study is to carefully investigate the speciation distribution of uranyl-chloride complex at elevated temperatures up to 500°C in acidic aqueous solutions, for a range of chloride concentrations, and to try and resolve the discrepancies between these two studies. The use of Raman spectroscopy for my study is especially useful because of the potential for direct

comparison between my results and those of Dargent *et al.* [1]. I used the hydrothermal diamond anvil cell (HDAC) as a sample containment vessel for my experiments.

Experimental Procedure

    Sample Preparation. For the preparation of aqueous uranyl sample containing chloride, 0.148 g of UO_3 powder, obtained from Los Alamos National Laboratory, was added slowly to 12.1 M HCl that was preheated to 150°C. The solution was stirred by slowly revolving the container in a circular fashion until a clear yellow solution was obtained. The resulting solution was evaporated slowly at 150°C in a period of about 2 hours and 30 minutes to obtain a yellow residue of $UO_2Cl_2.nH_2O$. This residue was then dissolved in deionized water in the presence of air to obtain a clear yellow solution with approximately 0.05 M uranium concentration. Then, 82.6 µl of 12.1 M HCl was added to acidify the solution (pH < 2), to avoid formation of uranyl hydrolysis species [17] and precipitation of uranates [5]. Finally, the chloride concentration was adjusted to set values (0.2, 1 and 3 M) by the addition of calculated amount of ultra-dry 99.9% LiCl powder (Alfa Aesar).

    A reference uranyl sample (Sample 1 A) was prepared to compare and calibrate the Raman data analysis process. The reference sample was prepared by dissolving UO_3 in trifflic acid as described below:

    A quantity of 0.22 g of UO_3, obtained from LANL, was taken in a test tube and about 3 ml of trifflic acid was added using a 1 ml pipette in small drops, while carefully shaking the test tube by hand. The solution was then sonicated for about 30 minutes after which a mostly clear solution with tiny amount of residue was obtained. The sample was then filtered through a 0.1 µm pore-size filter attached to a syringe, to get a clear yellow solution of uranyl in trifflic acid.

The solution was then diluted with about 2 ml of DI water to adjust the uranyl concentration close to 0.15 M.

The concentration of each of the solution samples studied in this project, and the temperature and pressure ranges used for each, are tabulated in Table 2.1.

Table 2.1: Specifications of the samples used in the Raman experiments.

Name	Concentration of Uranyl (M)	Concentration of Chloride (M)	Temperature range (°C)	Pressure range (MPa)
Sample 1A	0.15	0.0	25-300	VP – 530
Sample 2A	0.05	0.2	25-500	VP – 450
Sample 2B	0.05	1.0	25-500	VP – 450
Sample 2C	0.05	3.0	25-500	VP – 450

The High P-T Containment Cell. Acquisition of high-quality Raman spectrum is challenging for aqueous samples especially at high temperature and pressure conditions and is greatly influenced by the properties of the containment cell. Some of the most important characteristics required of the containment cell are: (a) The material of the cell must have enough mechanical strength to withstand the pressure and temperature conditions used in the experiment. (b) The material of the cell must be physically and chemically stable at all P-T conditions used in the experiment. (c) The material of the cell must be chemically inert with the experimental sample solution at all P-T conditions used in the experiment. (d) The material of the cell must be transparent in the visible region and must not produce fluorescence background. A high P-T containment cells satisfying all of the above requirements and possessing much versatility is the

hydrothermal diamond anvil cell (HDAC) developed by Bassett *et al.* [18]. The HDAC is fitted with resistive heaters and thermocouples so that it can control and maintain the temperature with an accuracy of ±0.5 °C [18]. Individual power sources (PHYWE, Germany) with output of 0-12 V dc and 0-5 A were used to supply power to the heaters. Multimeter thermometers (BK Tool Kit 2706) rated up to 750°C were used to measure the temperature of the sample. An HDAC is suitable for Raman spectroscopic measurements due to the transparent nature of diamonds in the visible region and because of its simple but precise working mechanism and relatively easier handling requirements. For additional details on the operation of the HDAC, the reader is referred to additional references [18]. For the best results, diamonds with the least level of background fluorescence were chosen. The acceptable level of fluorescence was determined by taking Raman spectra of the diamonds at different positions in the culet face and the inside of the diamonds and visual inspection of the spectra. In the experiment, I used the two-post version of the cell modified by Anderson *et al.* [19] and Yan *et al.* [20]. This version has the benefits of having better access to the sample space for sample loading and for the measurement probes [19], [20]. The sample volume is defined by two opposing 1/8 carat diamond anvils sandwiching a rhenium gasket, which has a circular hole milled in the center. Thus, the sample volume is cylindrical in shape and is formed by the inner walls of the hole in the gasket and the culet faces of the top and bottom diamond anvils. The rhenium metal and diamond are the only materials that come in contact with the sample during experiment and both are proven to be chemically inert and physically stable up to the maximum temperature and pressure used in our experiments [18]-[20]. The culet face of each diamond anvil measures 1mm in diameter. The rhenium gasket is 125 μm thick and has a circular hole of 500 μm diameter in the center. The uncompressed volume of the sample space is approximately 0.025 mm^3. Due to compression of the gasket upon

sealing and increase in pressure beyond ambient conditions, the experimental sample volume is somewhat reduced in comparison to the uncompressed volume. The aqueous samples were loaded in air and sealed to have a final density of about 0.75 to 0.8 g/cm^3. The approximate density of the fluid was determined by visual inspection of the size of air/vapor bubble after sealing and confirmed during the heating and cooling processes in the experiment by noting the liquid-vapor homogenization temperature (T_H). Once the T_H is known, assuming that the fluid follows the equation of state (EOS) of water with a permissible error margin [18], the density of the fluid is confirmed and the EOS of water for that specific density is used to calculate the pressure at each measurement temperature.

Raman Spectroscopic System and Spectra Acquisition. For the *in-situ* measurement of the Raman spectra of the aqueous uranyl-chloride solution samples, a Raman spectrometer (Labram HR 800, Jobin-Yvon, Horiba) coupled with a confocal microscope (Olympus) and solid-state diode laser (Laser Quantum) was used. The confocal nature of the system, which provides the ability to focus at specific depths of the sample and reject the scattered light coming from unfocused portions, was important for my work because of the need to focus the excitation source laser light at the center of the sample solution, to avoid the scattering of light from the diamond anvils. The wavelength of excitation source laser is 532 nm; the laser light was focused on the sample using a 20x magnification objective lens (Mitutoyo) having a working distance of 20 mm. An objective with a relatively longer working distance (20 mm) was required to access the sample which is positioned around the middle of the HDAC. The laser power delivered at the sample was approximately 30 mW during the experiments. For the best quality spectra, a 600 grooves/mm grating was used with a confocal hole diameter of 250 μm. The spectral resolution of the measurements was 1 cm^{-1}. After optimization of the signal/noise ratio for the spectra, by

obtaining the highest intensity of the uranyl v_1 Raman band and the achieving the best cancellation of background fluorescence, the spectra were collected with 30 accumulations of 60 seconds acquisition at each spectral window. The spectra were collected for the spectral window of 500 cm^{-1} to 1200 cm^{-1}, which avoids the diamond peak at about 1332 cm^{-1}. For each solution sample, Raman spectra were acquired first at room temperature (25°C ±1°C) and then at each temperature point in the following sequence: 100°C, 200°C, 300°C, 400°C and 500°C. The sample was allowed to thermally equilibrate for about 30 minutes before spectral acquisition was made at each temperature point.

Raman Spectra Fitting Procedure. The as obtained Raman spectra were background subtracted using polynomial of degree 3 and then averaged over 3-5 independent scans, each having identical acquisition settings (as described above), using Labspec5 software (Horiba). The averaged spectra were then processed further using OriginPro 8.5 commercial software (Origin Lab).

The spectra for Sample 1 A, the peaked band occurring at ~870 cm^{-1} and stemming solely from the (UO_2^{2+}) uranyl ion were fitted up to 250°C, where the Voigt function (a convolution of Gaussian and Lorentzian functions) gave the most accurate and consistent fit (Fig. 2.1). It should be mentioned that the UO_2^{2+} species is most likely an aqua ion complex of the form $UO_2(H_2O)_5^{2+}$. However, the band occurring at ~870 cm^{-1} stems from the U-O stretching mode vibration and the Raman signal is insensitive to the modes stemming from U- H_2O coordination. This also holds true for the aqueous uranyl chloride complexes, which are most likely of the aqua-chloro type, $UO_2(H_2O)_4Cl^+$, $UO_2(H_2O)_3Cl_2^0$, etc. At 300 °C, the uranyl peak is no longer symmetric, possibly due to complexation after decomposition of trifflic acid just below 300 °C,
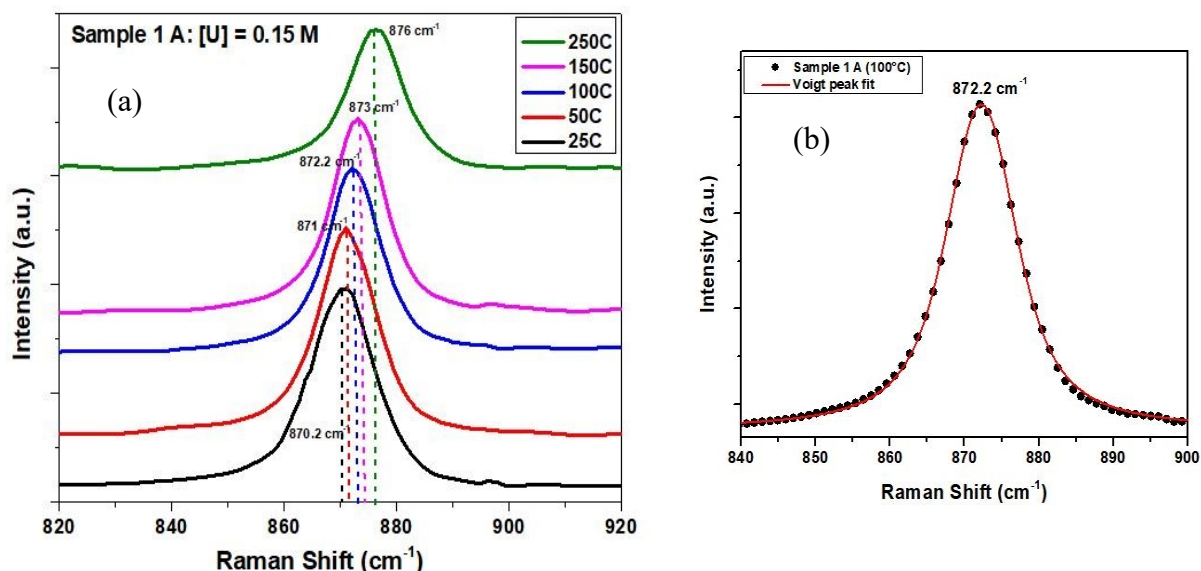
Fig. 2.1: Raman spectra of symmetric stretching vibrations of uncomplexed aqueous uranyl ion (Sample 1 A): (a) showing the gradual shift in peak position towards higher wavenumbers (blue-shift) with increasing temperature, and (b) showing the Voigt function fitted spectra at 100 °C.

and hence not used for fitting purposes. The Voigt function was then universally used in fitting all of the Raman spectra measured at up to high temperatures for all the samples. The peak position (i.e., centroid) for the uranyl ion shows a small gradual shift towards higher wavenumbers with increasing temperature (Fig. 2.1), which agrees with the findings from the Dargent *et al.* study [1]. The average full-width-half-maximum (FWHM) of the uranyl peak was about 13 cm^{-1} and some broadening at higher temperature was observed, but a clear trend could not be deduced. These variations in peak position and the FWHM with temperature were considered during the fitting procedure of Raman bands for the chloride-bearing aqueous solution (2A – 2C) samples.

The Raman bands of samples containing chloride complexes at elevated temperatures were modelled using the method of self-consistency and physical relevance. I used the set of least number of peaks with consistent peak position that could consistently fit the data, within

reasonable error, for all temperature and concentration range explored in our experiment. This was an iterative process and took several iterations to achieve the final fit. During this process, the position and FWHM of the Uranyl peak were constrained around the values obtained from the corresponding temperature for the reference sample and all other parameters were allowed to vary. Several different sets of parameters were explored, and the inconsistent fits were eliminated, after which, the consistent ones were refined, from which the most consistent fit was chosen and further refined to finally get the fit with least possible error and best physical interpretation. This fitting procedure gave me peak positions and FWHM for the uranyl chloride complexes that are in general agreement with the corresponding behavior of the uranyl ion; A similar gradual shift towards higher wavenumbers for each species with increase in temperature and some peak broadening at higher temperatures. Table 2.2 summarizes the key parameters determined from the peak fitting procedure described above.

Table 2.2: Parameters (peak positions and FWHM) determined for various uranyl-chloride complex species from peak fitting of Raman spectra.

Species	Average FWHM (cm^{-1})	Raman Vibrational frequency in cm^{-1}					
		25°C	100°C	200°C	300°C	400°C	500°C
UO_2^{2+}	13.9	870.8	870.9	872.6	-	-	-
UO_2Cl^+	16.5	861.5	861.7	862.6	862.5	862.4	862.6
$UO_2Cl_2^0$	16.1	849.5	849.9	851.5	852.2	852.7	852.9
$UO_2Cl_3^-$	16.5	-	-	840	840.6	841.2	841.5

Results

Fig. 2.2 (a) shows the evolution of the Raman band profile with temperature for Sample 2C (3 M Cl$^-$). In contrast to the behavior of Sample 1A (UO$_2$$^{2+}$), here, the band profile gradually shifts towards lower wavenumber with increase in temperature. This decrease in the
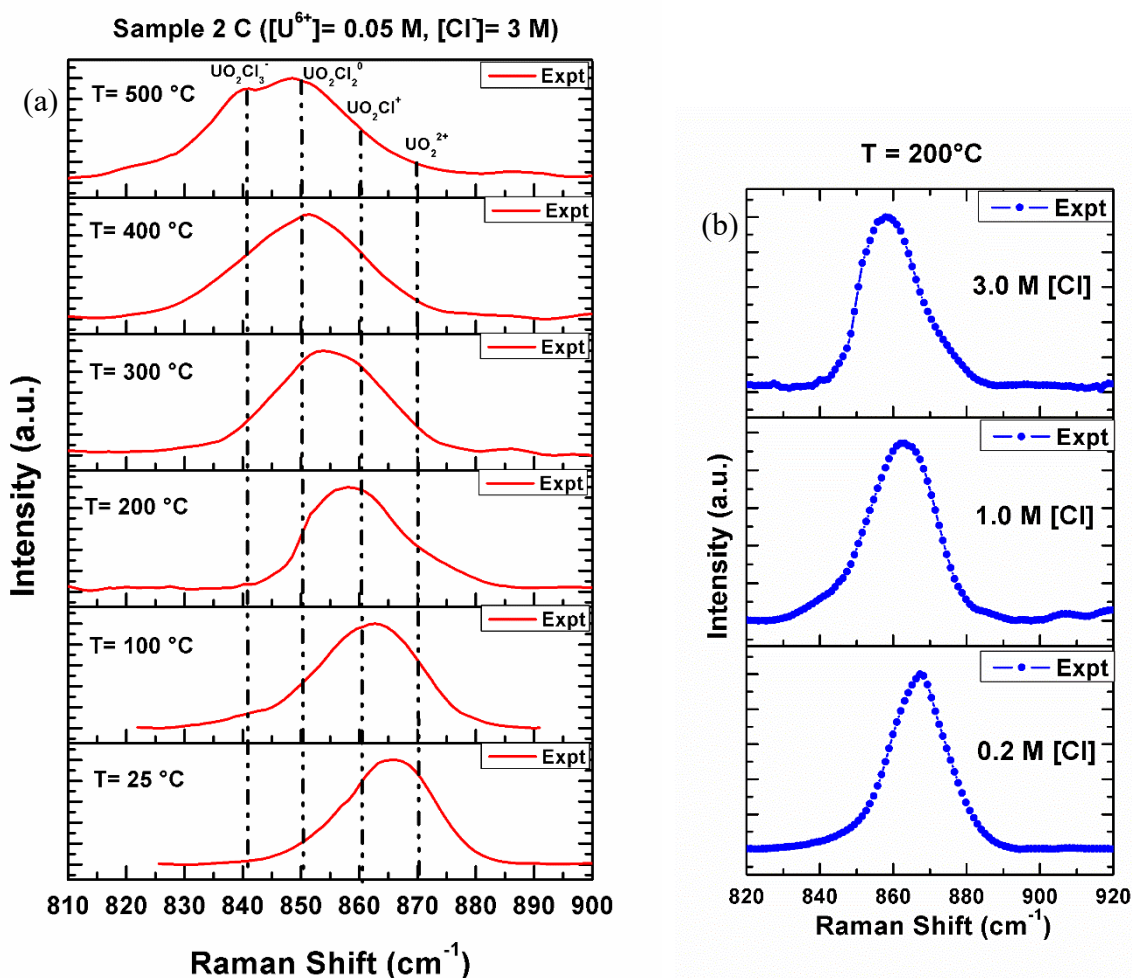

Fig. 2.2: Evolution of the symmetric Raman vibrational band of uranyl ion with: (a) temperature for Sample 2 C and (b) chloride concentration at 200 °C.

mean wavenumber of the overall band occurring within the range from ~830 to ~880 cm^{-1}, is clearly evident despite the fact that the peak position of individual specie in the complex

generally shifts towards higher wavenumber with increase in temperature. The decrease is due to the changing relative contribution of different uranyl chloride complex species to the overall band, with increase in temperature. Similar evolution of the Raman band towards lower wavenumbers is also noticed with increase in chloride concentration at a given temperature, which is also due to the uranyl chloride complex speciation change with chloride concentration. Fig. 2.2 (b) shows the evolution of Raman band with changing chloride concentration at 200°C.

Using the peak fitting procedure described in previous section, I was able to fit the Raman spectra for the whole range (Table 2.1) of temperature and chloride concentration used in my experiment, with a maximum of 4 different peaks, positioned approximately at 870 cm^{-1}, 860 cm^{-1}, 850 cm^{-1} and 840 cm^{-1}. The overall fitted Raman band, being comprised of the individual v_1 symmetric stretching vibrations of the O=U=O bond of the UO_2^{2+}, UO_2Cl^+ and $UO_2Cl_2°$, etc., complexes for the 2A - 2C solutions are shown in Fig. 2.3. These four peaks were sufficient to fit each of the obtained spectra, and each of the peaks exhibit similar gradual shift towards higher frequency (as shown in Fig. 2.4) and some peak broadening with increase in temperature, as was seen with the uncomplexed UO_2^{2+} (Sample 1A). The peak at about 870 cm^{-1} is identified with the band of the UO_2^{2+} ion whereas the three additional peaks occurring at approximately 860 cm^{-1}, 850 cm^{-1} and 840 cm^{-1} are assigned to the bands of the UO_2Cl^+, $UO_2Cl_2^0$ and $UO_2Cl_3^-$ species, respectively. The Raman vibrational frequency and FWHM values for each of these species, obtained from fitting of the Raman spectra measured at temperatures ranging from 25 to 500°C and averaged over all concentrations, are summarized in Table 2.2.

Fig. 2.3: Showing the fitted peaks for the Raman spectra of aqueous uranyl samples 2A – 2C for temperatures 25 °C – 500°C.

As seen in Table 2.2, at any given temperature (from top to bottom on each column), the vibrational frequencies of species of the complex decrease with increase in number of chloride ligands attached to them. This monotonous shift in position to lower wavenumber, of the uranyl vibration maximum of the species of uranyl chloride complex with the increase in number of chloride ligands in the complex can be quantified using a simple equation:

$$v1 = -nA + 870(\pm 1) \quad \text{--- (1)}$$
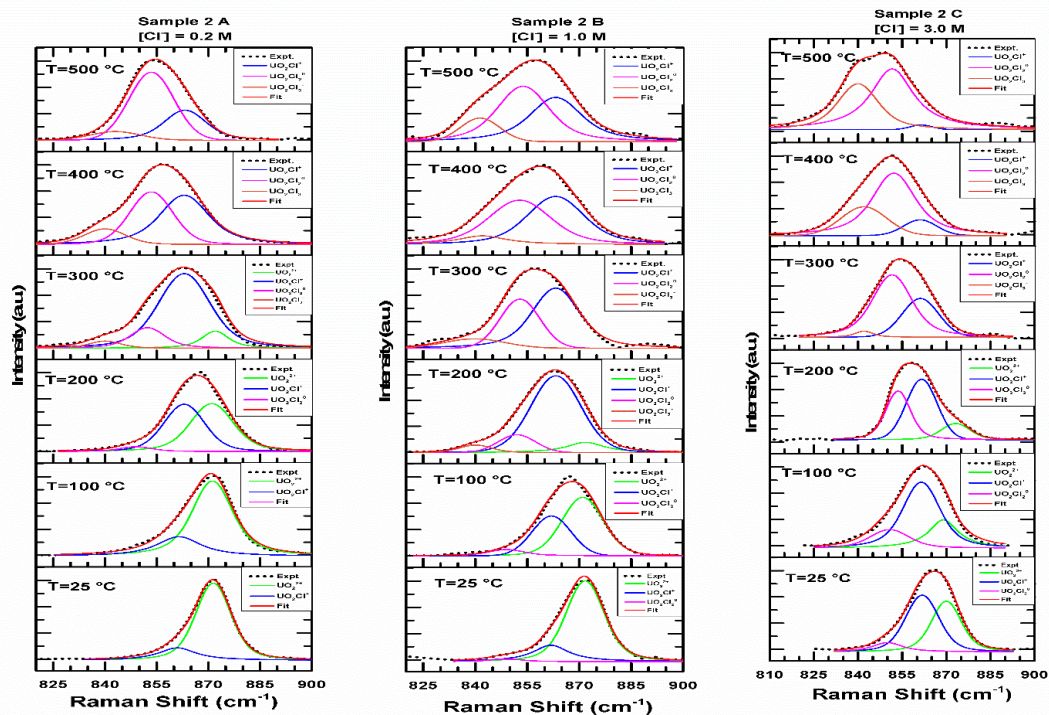
Where, v_1 is the vibrational frequency (in cm^{-1}) of the specie, n is the number of chloride ligands and A is the average shift (in cm^{-1}) per chloride added to the complex. This equation was
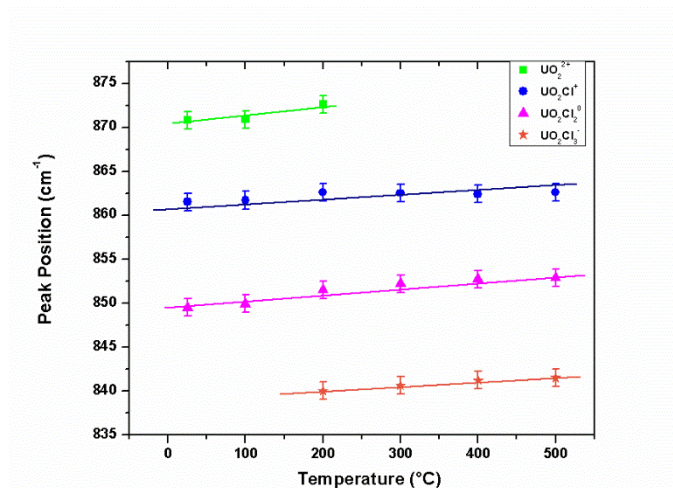
Fig. 2.4: Graph of average peak position of various species of the uranyl-chloride complex plotted against temperature, showing linear trend (not a linear-fit) in blue-shift with increasing temperature seen for all of the species in the complex.

previously used by Nguyen-Trung *et al.* [21] to quantify the shift per ligand corresponding to different ligands of interest. In this study, the value of A in equation 1 was calculated to be 10.2 ($\pm$1) cm^{-1} per chloride ligand added to the complex, using the results from fitting of Raman spectra obtained from samples having different chloride concentration (2A, 2B, and 2C) and for all temperatures ranging from 25 to 500°C. This calculation is illustrated in Table 2.3.

Table 2.3: Calculation of average red-shift of the intensity maxima per chloride ligand.

Species	Peak position averaged over whole temperature range (cm^{-1})	No. of chloride ligands n	Average shift per ligand A (cm^{-1})	Average value of A (cm^{-1})
UO_2^{2+}	871.4	0	-	
UO_2Cl^+	862.2	1	9.2	
$UO_2Cl_2^0$	851.4	2	10.8	10.2
$UO_2Cl_3^-$	840.8	3	10.6	

Assuming that the Raman scattering cross section of every species in the complex are comparable, within reasonable error, the area under each peak corresponding to a particular specie in the complex can be used to compare the relative contribution of each specie to the whole Raman band. This relative contribution will be directly proportional to the amount of each specie present in the complex under those conditions. The amount (in percentage) of each specie present in the complex are plotted against temperature for solutions 2A, 2B and 2C in Fig. 2.5.
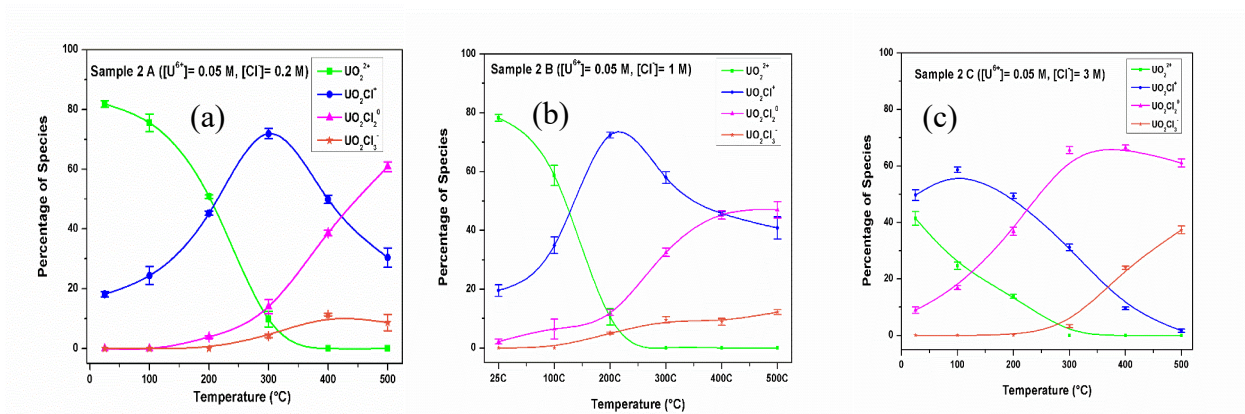
Fig. 2.5: Speciation distribution (in percentage) of aqueous uranyl-chloride solutions plotted against temperature of the solution for different chloride concentrations: (a) 0.2 M, (b) 1 M and (c) 3 M

At lower temperature and lower chloride concentration the dominant specie is the UO_2^{2+} ion, whereas, with increase in temperature and chloride concentration, complexes such as UO_2Cl^+ and $UO_2Cl_2^0$ dominate, indicating the increase in chloride ligation number with increase in temperature and chloride concentration. This is because of the increasing activity of chloride ions at higher temperature. This phenomenon is also consistent with the known properties of hydrothermal solutions. Due to the decrease in dielectric constant of water as it approaches towards supercritical conditions at higher temperature, its dielectric polar property is lost,

meaning water can no longer provide efficient shielding of the charged species, and as a consequence, the more-neutral ones are favored at higher temperature. For the sample having 0.2 M chloride concentration (Fig. 2.5 (a)), the dominance of UO_2^{2+} gradually decreases from room temperature and vanishes at about 300°C, whereas, UO_2Cl^+ becomes more prominent and peaks at around 300°C, which fades away with further increase in temperature. From 300°C, $UO_2Cl_2^0$ emerges and rises in prominence as the temperature is further increased. For 1 M chloride solution (Fig. 2.5 (b)), similar behavior observed but at lower temperatures; UO_2^{2+} speciation reaches zero percent around 200°C whereas UO_2Cl^+ speciation peaks at ~200°C. This trend is further extended to the 3 M chloride solution where UO_2^{2+} speciation is very low even at room temperature and UO_2Cl^+ speciation peaks around 100°C. Beyond about 250°C, the speciation is dominated by $UO_2Cl_2^0$ with some $UO_2Cl_3^-$ at higher temperatures. In general, the number of chloride ligands associated with each uranyl ion increases with increase in temperature and with increase in chloride concentration (0.2 M, 1 M, 3 M). Furthermore, the speciation is dominated by the neutral specie $UO_2Cl_2^0$ at higher temperatures (above 400°C) with some contribution from singly charged species, UO_2Cl^+ at lower chloride concentration (0.2 M and 1 M) and $UO_2Cl_3^-$ at higher chloride concentration (3 M). This is more easily observed in the plots of percentage contribution of each species vs chloride concentration in the aqueous solution at constant temperature (25, 200 and 400°C), as shown in Fig. 2.6.

At room temperature (Fig. 2.6 (a)), the UO_2^{2+} species is dominant in most of the concentration range explored in this study. This is not the case at 200°C (Fig. 2.6 (b)), where UO_2Cl^+ is dominant with some contribution from UO_2^{2+} at lower chloride concentrations and $UO_2Cl_2^0$ at higher chloride concentrations. At 400°C (Fig. 2.6 (c)), the speciation is dominated by the neutral specie $UO_2Cl_2^0$, which contributes more than 40% to the overall speciation at all
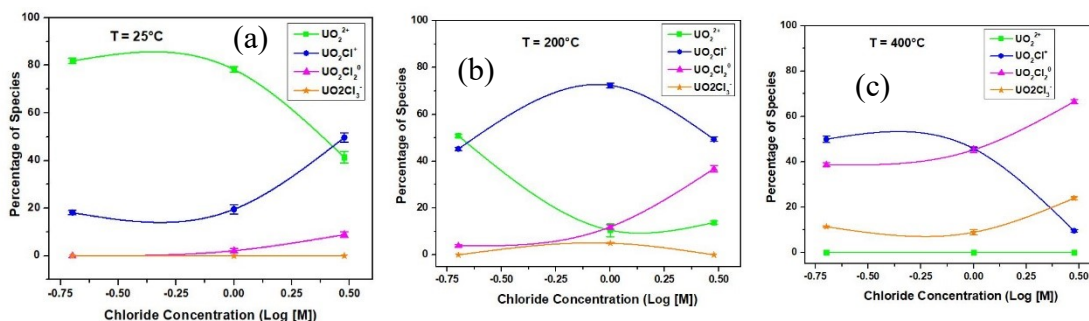
Fig. 2.6: Speciation distribution (in percentage) of aqueous uranyl-chloride solutions plotted against chloride concentration in the solution at: (a) 25 °C, (b) 200 °C and (c) 400 °C.

concentrations studied. This shows a clear picture of the speciation distribution of the aqueous complex of uranyl chloride under hydrothermal conditions. Under such conditions; UO_2^{2+} is the most abundant specie at room temperature, more prominently at lower chloride concentrations; UO_2Cl^+ dominates speciation at temperatures around 200°C and $UO_2Cl_2^0$ prevails above 400°C for the concentration range studied here. The contribution to the speciation of the negatively charged specie, $UO_2Cl_3^-$, is only noticeable at 500°C and 3 M chloride concentration.

Discussion

Previous work on the aqueous uranyl chloride system at high temperature and pressure conditions is limited to only two studies; Dargent *et al.* [1] and Migdisov *et al.* [3]. These two studies were made using different characterization techniques and ended up with two sets of contrasting results. As a key difference, the speciation distributions obtained by these two groups differ significantly; Migdisov *et al.* [3] identified the species UO_2^{2+}, UO_2Cl^+, $UO_2Cl_2^0$ and some of $UO_2Cl_3^-$ measured at up to 250°C, whereas, Dargent *et al.* [1] found (study made to 350 °C), in addition to the species identified by Migdisov *et al.* [3], highly charged species like $UO_2Cl_4^{2-}$ and $UO_2Cl_5^{3-}$ and one additional specie that they were not able to identify, in uranyl chloride

solutions having very similar chloride concentrations. Our speciation distribution results show the presence of UO_2^{2+}, UO_2Cl^+, $UO_2Cl_2^0$ and some of $UO_2Cl_3^-$, with UO_2Cl^+ and $UO_2Cl_2^0$ dominating the higher temperature range in nearly identical aqueous solutions. Our results align more closely with those of Migdisov et al. [3].

Assuming negligible differences due to the spectroscopic cells, Raman instruments and other external experimental factors on the Raman spectra measured from the uranyl chloride aqueous samples, the only significant discrepancy between the procedures used in my study and that made by Dargent et al. [1] is the spectral analysis procedure used to fit the experimental data. In their model, they used the peak position for the uranyl chloride complex species speculated by Nguyen-Trung et al. [21], who considered the presence of highly charged (negative) species in aqueous uranyl solutions covering a wide range of chloride concentrations. According to Nguyen-Trung et al. [21], the average shift of the peak is just about 4 cm^{-1} per chloride ligand added to the complex. Use of this shift and the peak positions resulted in very sharp peaks with uniform FWHM values of 5.5 cm^{-1} for all species and temperature range. Dargent et al. [1] applied the same analysis approach proposed by Nguyen-Trung et al. [21], which resulted in a scattered speciation distribution that is not physically realistic and is lacking internal self-consistency, in their study. For example, they did not see the shift of peak position towards higher frequency with increase in temperature for the uranyl chloride species, even though they report seeing a monotonic blue-shift of the UO_2^{2+} stretching mode vibration band peak. In contrast, I used a different and more physically acceptable model for hydrothermal conditions, where lower charged species (i.e., trending toward neutrality) are more stable in the aqueous environment at higher temperature. Furthermore, in my study, the peak position and FWHM used for the species in the complex were not constrained, except for the uranyl ion

whose parameters were known from the analysis of spectra from the reference sample (1A).

Although not completely monotonic, I noticed some peak broadening for each of the species in

the complex towards higher temperatures. More importantly, I observed a nearly linear and

identical blue-shift of the peaks corresponding to each of the uranyl chloride species (see Fig.

2.4). In developing an equation similar to the one given by Nguyen-Trung *et al.* [21] for

modelling the peak red-shift due to addition of each chloride ligand to the uranyl chloride

complex, I calculated the value for *A* (which gives the average red-shift per chloride ligand

added) in the equation to be 10.2 ± 1 cm^{-1}. It should be noted that this shift calculated in my

experiment is in close agreement to the values computed in a theoretical study [22], which

investigated the vibrational frequencies of the species of aqueous uranyl chloride complex,

despite the absolute values of the peak positions not being in complete agreement with my

experimental values. Furthermore, my speciation model used for the fitting of Raman spectra

gave a smooth and physically realistic speciation distribution, which agrees well with the results

obtained by Migdisov *et al.* [3] using UV-Vis spectroscopy to measure essentially an identical

system of aqueous solutions.

It should be mentioned that Nguyen-Trung *et al.* [21] reported that they did not see any

$UO_2Cl_4{}^{2-}$ or $UO_2Cl_5{}^{3-}$ species in the experiments with the same sample using UV-Vis

spectroscopy. Also, they only identified the species with up to 3 chloride ligands in the complex

when they used $(CH_3)_4NCl$ in place of LiCl to adjust chloride concentration and they conjecture

that the complexation must be limited to tri-chloro species.

One can generally fit two peaks in place of a single peak, but the reverse may not be

always true. In any case, the least number of peaks that can fit a set of data consistently is

generally the best fit. It is likely that Dargent *et al.* [1] overparameterized the fitting procedure to

match the peak position as suggested by Nguyen-Trung *et al.* [21] and consequently inserted

more than necessary peaks to fit the experimental data. As they note in their paper, a maximum

of 4 intensity peaks were visible for data at 250°C (Fig. 2.7) [1], and looking at the data it
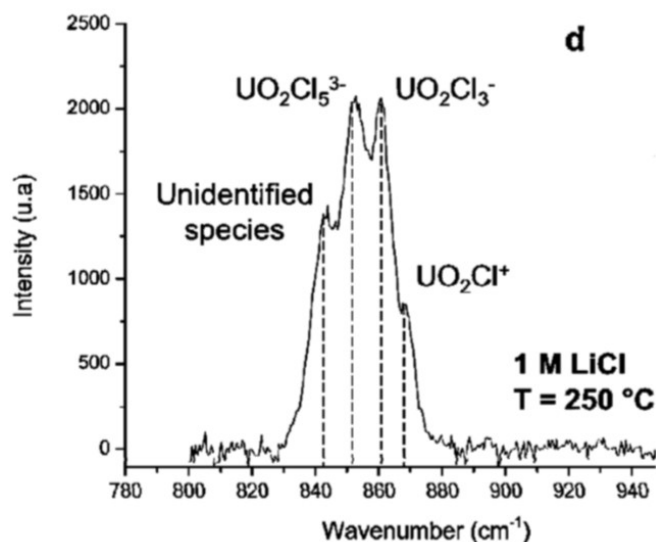
Fig. 2.7: Data from Dargent *et al.* [1], showing the Raman spectra of aqueous uranyl complex at
250 °C and 1 M chloride concentration, with 4 intensity maxima.

seems it could well be fitted with only those 4 peaks and that would generally agree with the

number and approximate position of the peaks from my peak fitting results. The additional small

peaks added in between the prominent ones, it seems, were in most part to minimize the error in

peak fitting and to be consistent with the peak positions given by Nguyen-Trung *et al.* [21].

However, it would be very difficult and controversial, without the prior knowledge of speciation

from other techniques, to assign a particular specie, without much error, for each peak position

that are only about 4 cm^{-1} apart from each other, just from a convoluted Raman band having

multiple components. Comparing the peak positions determined in my study to the ones

delineated by Dargent *et al.* [1] in Fig. 2.7, the positions generally seem to match except for the

additional peaks. For example, if the data shown in Fig. 2.7 are fitted with only those 4 peaks visible in the spectrum, the assignments would correspond to UO_2^{2+}, UO_2Cl^+, $UO_2Cl_2^0$ and $UO_2Cl_3^-$ from right to left, which would approximately match my results. In addition, the peak at around 841 cm^{-1} coded as 'unidentified species' by Dargent *et al.* [1], would then be identified as corresponding to the specie $UO_2Cl_3^-$.

Conclusion

This is the first study on the speciation of aqueous uranyl chloride complexes under hydrothermal conditions performed from 25 to 500°C; previous studies only extended to 350°C. Raman spectra were collected for uranyl chloride complex from a hydrothermal solution contained in a HDAC. The Raman band of the symmetric stretching vibration mode of the O=U=O bond shows a systematic evolution, both with temperature and chloride concentration. This evolution in the band is attributed to the evolving contribution of individual uranyl chloride species to the total band with changing temperature or chloride concentration. These contributions were quantified by fitting the Raman spectra measured at each temperature and for each chloride concentration within the aqueous solution. From this fitting, the important peak parameters such as peak position and FWHM were determined, and the uranyl chloride speciation distributions were obtained for all temperatures and chloride concentrations in aqueous solutions of the study. The speciation distributions thus obtained were compared with previous studies made on the same system and the similarities and differences were discussed.

Acknowledgements

References

[1] M. Dargent, J. Dubessy, L. Truche, E. F. Bazarkina, C. Nguyen-Trung, and P. Robert, "Experimental study of uranyl(VI) chloride complex formation in acidic LiCl aqueous solutions under hydrothermal conditions (T= 21 C–350 °C, Psat) using Raman spectroscopy," *European Journal of Mineralogy*, vol. 25, no. 5, pp. 765–775, Oct. 2013.

[2] X. Liu, J. Cheng, M. He, X. Lu, and R. Wang, "Acidity constants and redox potentials of uranyl ions in hydrothermal solutions," *Physical Chemistry Chemical Physics*, vol. 18, no. 37, pp. 26040–26048, 2016.

[3] A. A. Migdisov, H. Boukhalfa, A. Timofeev, W. Runde, R. Roback, and A. E. Williams-Jones, "A spectroscopic study of uranyl speciation in chloride-bearing solutions at temperatures up to 250 °C," *Geochimica et Cosmochimica Acta*, vol. 222, pp. 130–145, Feb. 2018.

[4] Oreskes and Einaudi, "Origin of hydrothermal fluids at Olympic Dam; preliminary results from fluid inclusions and stable isotopes," *Economic Geology, GeoScienceWorld,* 1992. [Online]. Available: https://pubs.geoscienceworld.org/segweb/economicgeology/article-abstract/87/1/64/21011. [Accessed: 17-Mar-2019].

[5] A. Richard, C. Rozsypal, J. Mercadier, D. A. Banks, M. Cuney, M. Boiron, and M. Cathelineau, "Giant uranium deposits formed from exceptionally uranium-rich acidic brines," *Nature Geoscience*, vol. 5, p. 142, Dec. 2011.

[6] M. Cuney, "The extreme diversity of uranium deposits," *SpringerLink,* 2009. [Online]. Available: https://link.springer.com/article/10.1007%2Fs00126-008-0223-1. [Accessed: 17-Mar-2019].

[7] Derome, "Mixing of sodic and calcic brines and uranium deposition at McArthur river, Saskatchewan, Canada: A Raman and laser-induced breakdown spectroscopic study of fluid inclusions," *Economic Geology, GeoScienceWorld,* 2005. [Online]. Available:

https://pubs.geoscienceworld.org/segweb/economicgeology/article-abstract/100/8/1529/127679. [Accessed: 17-Mar-2019].

[8]   L. Kish and M. Cuney, "Uraninite-albite veins from the Mistamisk Valley of the Labrador Trough, Quebec," *Mineralogical Magazine*, vol. 44, no. 336, pp. 471–483, Dec. 1981.

[9]   M. Z. Min, X. Z. Luo, and S. L. Mao, "The Saqisan Mine — a paleokarst uranium deposit, South China," *ScienceDirect,* 2002. [Online]. Available: https://www.sciencedirect.com/science/article/pii/S016913680000010X. [Accessed: 17-Mar-2019].

[10]   K. J. Wenrich and S. R. Titley, "Uranium exploration for northern Arizona (USA) breccia pipes in the 21st century and consideration of genetic models," p. 16, 2009.

[11]   R. Guillaumont, T. Fanghanel, J. Fuger, and I. Grenthe, "Guillaumont: Update on the chemical thermodynamics," *Google Scholar,* 2003. [Online]. Available: http://www.wipp.energy.gov/library/cra/2009_cra/references/Others/Guillaumont_et_al_20 03_Update_on_Chemical_Thermodynamics.pdf. [Accessed: 17-Mar-2019].

[12]   S. Ahrland, "On the complex chemistry of the uranyl ion," *Acta chemica scandinavica*, 1951.

[13]   Choppin and Du, "f-Element complexation in brine solutions," *Radiochimica Acta*, 1992.

[14]   Davies and Monk, "Spectrophotometric studies of electrolytic dissociation. Part 4.—Some uranyl salts in water," *Transactions of the Faraday Society (RSC Publishing)*, 1957.

[15]   Soderholm, "Structural correspondence between uranyl chloride complexes in solution and their stability constants," *The Journal of Physical Chemistry A (ACS Publications),* 2011. [Online]. Available: https://pubs.acs.org/doi/10.1021/jp111551t. [Accessed: 17-Mar-2019].

[16]   C. Hennig, J. Tutschku, A. Rossberg, and A. C. Scheinost, "Comparative EXAFS investigation of Uranium (VI) and -(IV) aquo chloro complexes in solution using a newly developed spectroelectrochemical cell," *Inorganic Chemistry (ACS Publications),* 2005. [Online]. Available: https://pubs.acs.org/doi/abs/10.1021/ic048422n. [Accessed: 17-Mar-2019].

[17]   T. Fujii, K. Fujiwara, H. Yamana, and H. Moriyama, "Raman spectroscopic determination of formation constant of uranyl hydrolysis species (UO2)2(OH)22+," *Journal of Alloys and Compounds*, vol. 323–324, pp. 859–863, Jul. 2001.

[18]   W. A. Bassett, A. H. Shen, M. Bucknum, and I. Chou, "A new diamond anvil cell for hydrothermal studies to 2.5 GPa and from −190 to 1200 °C," *Review of Scientific Instruments*, vol. 64, no. 8, pp. 2340–2345, Aug. 1993.

[19] A. J. Anderson, H. Yan, R. A. Mayanovic, G. Solferino, and C. J. Benmore, "High-energy X-ray diffraction of a hydrous silicate liquid under conditions of high pressure and temperature in a modified hydrothermal diamond anvil cell," *High Pressure Research*, Vol 34, no. 1, 2014.

[20] H. Yan, R. A. Mayanovic, A. J. Anderson, and P. R. Meredith, "An in situ X-ray spectroscopic study of Mo6+ speciation in supercritical aqueous solutions," *Nuclear Instruments and Methods in Physics Research Section A: Accelerators, Spectrometers, Detectors and Associated Equipment*, vol. 649, no. 1, pp. 207–209, Sep. 2011.

[21] C. Nguyen-Trung, G. M. Begun, and Donald A. Palmer, "Aqueous uranium complexes. 2. Raman spectroscopic study of the complex formation of the dioxouranium (vi) ion with a variety of inorganic and organic ligands," *Inorg. Chem.*, 31, 5280-5287, 1992.

[22] F. Izquierdo-Ruiz, J. M. Menéndez, and J. M. Recio, "Theoretical analysis of vibrational modes in uranyl aquo chloro complexes," *Theoretical Chemistry Accounts*, vol. 134, no. 2, Feb. 2015.

CHAPTER 2: DESIGN OF A CONTAINMENT APPARATUS FOR SYNCHROTRON XAS MEASUREMENTS OF RADIOACTIVE FLUID SAMPLES UNDER HIGH TEMPERATURES AND PRESSURES

Abstract. The simple working principles and versatility of the hydrothermal diamond-anvil cell (HDAC) make it highly useful for synchrotron x-ray studies of aqueous and fluid samples to high pressure-temperature (P-T) conditions. However, safety concerns need to be overcome in order to use the HDAC for synchrotron studies of aqueous radioactive samples to high temperatures and pressures. For accomplishment of such hydrothermal experiments of radioactive materials in synchrotron beamlines, the samples are required to be enclosed in a containment system employing three independent layers of airtight sealing while enabling access to the sample using several experimental probes, including incoming and outgoing x-rays. In this article, I report the design and implementation of a complete radiological safety enclosure system for an HDAC specialized for high P-T x-ray absorption spectroscopy (XAS) measurements of aqueous solutions containing the actinides at synchrotron beamlines. The enclosure system was successfully tested for x-ray absorption spectroscopy experiments using the HDAC with aqueous samples containing depleted uranium at temperatures ranging from 25 to 500 °C and pressures ranging from vapor pressure to 350 MPa.

Introduction

Studies of aqueous fluid (liquid, vapor or supercritical fluid) samples containing radioactive elements to high temperatures and pressures are critical in addressing a range of issues concerning actinides, including high-level waste disposal in underground repositories [1]–[4] and development of accident-tolerant nuclear fuels [5]–[7]. The hydrothermal diamond-anvil

cell (HDAC) has been proven to be a highly suitable instrument for synchrotron x-ray absorption spectroscopy (XAS) studies of aqueous solutions to high P-T conditions [8]. Previous synchrotron XAS investigations using the HDAC cover a wide range of elements that nevertheless exclude the actinide series and, thus, have not dealt with potential radiological containment issues. For my XAS investigations of actinide complexing in high P-T aqueous fluids, extreme care must be taken while containing radioactive fluid samples in a HDAC because of the possibility of radiological contamination due to leakage or failure, especially at higher P-T conditions. The US Department of Energy (DOE) synchrotron facilities, such as the Advanced Photon Source (APS) and the Stanford Synchrotron Radiation Laboratory (SSRL) stipulate that three independent layers of containment are required for running experiments on radioactive fluid samples in high P-T cells. For such experiments, an airtight enclosure with fitted, sealed feedthroughs for the heater and thermocouple wires having the capacity to contain the entire HDAC is needed. In addition, the enclosure must have clear paths for the incoming and outgoing x-rays for the XAS measurement. Moreover, such an enclosure should also have the provision for in and out flow of a reducing gas required during high temperature experiments with HDAC to prevent oxidation of cell components and the diamond anvils. To address these requirements for performing experiments on radioactive samples using the HDAC in synchrotron beamlines, I have devised a containment vessel and tested it in the experimental setup, which will be described in detail in this paper. The test experiments were performed with an aqueous solution bearing depleted uranium to high P-T conditions at beamlines 20-ID-C at the APS and 11-2 at SSRL.

HDAC

The central components of the HDAC developed by Bassett *et al.* [9] consist of two opposed 1/8 carat diamonds that are mounted on seats typically made of tungsten carbide or silicon nitride. The seats are wound with resistance heaters, made from molybdenum wires, that are used to heat the sample and are mounted on an upper and a lower platen (see Fig. 3.1 a). The platens are advanced toward one another by screws and guided by rods. Type K chromel-alumel thermocouples are placed in contact with the upper and lower diamond anvils and are used to measure the temperature of the sample. A correction typically needs to be made for the difference in temperature between the sample and the diamond anvils. This correction is calibrated using the melting points of sodium nitrate (306.8 °C) and sodium chloride (800.1 °C), and the α-β phase transition point of quartz (573 °C at 0.1 MPa). Because the sample size is small and due to the high thermal conductivity of diamond, the temperature gradient between sample and diamond anvils is small (≤2 °C). The temperatures are considered to be accurate to ±5 °C. Here, I use our modified two-post HDAC that was described elsewhere [10], [11]. As discussed previously [10], [11], the two-post design has principal advantages of smaller size and considerably greater sample accessibility, either for incoming x-rays or outgoing signal radiation, over the three-post HDAC originally developed by Bassett *et al.* [9].

A sample consisting of an aqueous liquid plus vapor bubble is placed in the sample chamber, defined by the 700 μm hole milled at the center of a 125 μm thick Rhenium (Re) gasket having an outer diameter of 3000 μm, and the two diamond-anvils that are compressed against the gasket. It was necessary to use nano-polycrystalline diamonds (NPD) due to the strong and copious Bragg peaks evident in the XAS signal when using type II-a crystalline diamonds. The lower NPD anvil has a sample recess ~500 μm in diameter and ~120 μm deep located in the

36

center of the culet face measuring 2000 μm across, whereas the upper anvil has a flat culet face. The sample recess was utilized in order to increase the sample excitation volume for the XAS measurements, which is approximately doubled using the experimental configuration described in further detail below.

The HDAC Enclosure

As outlined above, the use of an enclosure in my experiments serves to fulfill the radiological safety requirements of the APS and SSRL, for measurements of radioactive aqueous samples at high P-T conditions using the HDAC at synchrotron beamlines. As shown in Fig. 3.1(d), my enclosure serves as the third and outermost layer of the three-layer containment of the radioactive sample. The first two layers of the enclosure consist of the sample chamber and the Kapton tape covering the cylindrical stainless-steel collar (Figs. 3.1(b) and (c)) and the access/view ports along the loading axis of the cell, respectively. Fig. 3.2 shows a schematic diagram of the HDAC-enclosure assembly. Fig. 3.3 shows the components that make up the enclosure for the HDAC: Fig. 3.3(b) through e) show roughly the sequence of steps used to anchor and seal the sample-loaded HDAC inside the enclosure. The enclosure is made in a simple rectangular geometry for the container and lid design. The container and lid of the enclosure were machined from individual blocks of aluminum to avoid joints and to ensure perfect sealing. A 0.5 mm thick 100% silicone rubber gasket is used to seal the container and lid of the enclosure together using 2 mm diameter screws (see Fig. 3.3). The silicone sheet used for the gasket is rated for >200 °C temperature. Three 5 x 4 cm windows are milled in the container portion, two opposing windows on the side and one on the bottom, and one 5 x 4 cm window in the lid portion of the enclosure. The windows on the bottom of the container and on the lid are
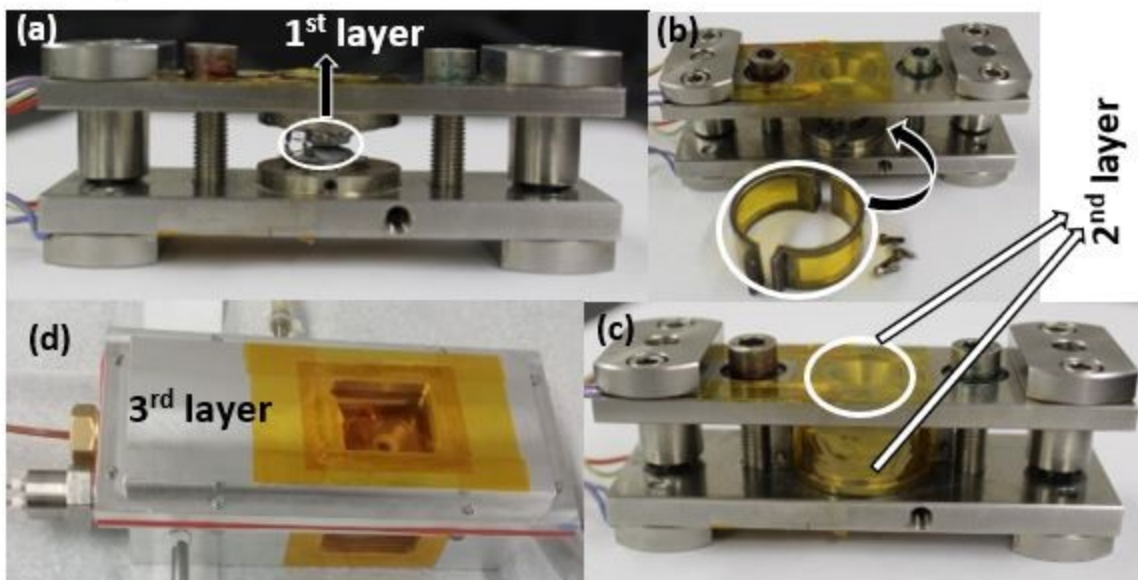
Fig. 3.1: Photographs showing three layers of sample containment: (a) the first layer encompasses the hole in the rhenium gasket and the diamond anvils that are pressed against the gasket from top and bottom, (b) the second layer consist of the collar (covered with Kapton film) and Kapton tape affixed over the viewports of the HDAC, (c) the collar shown in place in the cell, and (d) the third layer is the aluminum enclosure described in detail in section III of this article.

opposing and are oriented along the path of the incident x-ray beam. The windows on the sides

of the container are also opposing and allow for the detection of fluorescence x-rays emitted

from the gasket side (i.e., perpendicular to the loading axis of the cell) of the sample.

Furthermore, each of the windows is sealed from both sides (i.e., inside and outside of the

container and lid) using a single layer of 0.05 mm thick Kapton film, that is made to adhere using

high-temperature Loctite epoxy glue and Kapton tape. Two 4 mm diameter threaded holes are

tapped and fitted with 4 mm diameter hollow aluminum tubes on the opposing sides of the

container of the enclosure, serving as an inlet and outlet port for reducing gas (e.g., forming gas).

The gas line, starting from the regulated cylinder containing the reducing gas, is fitted with a

shut-off valve and a 1.5 psi rated pressure relief valve prior to the connection made at the

container part of the enclosure. In addition, a HEPA filter (ETA Filters), with a filter efficiency
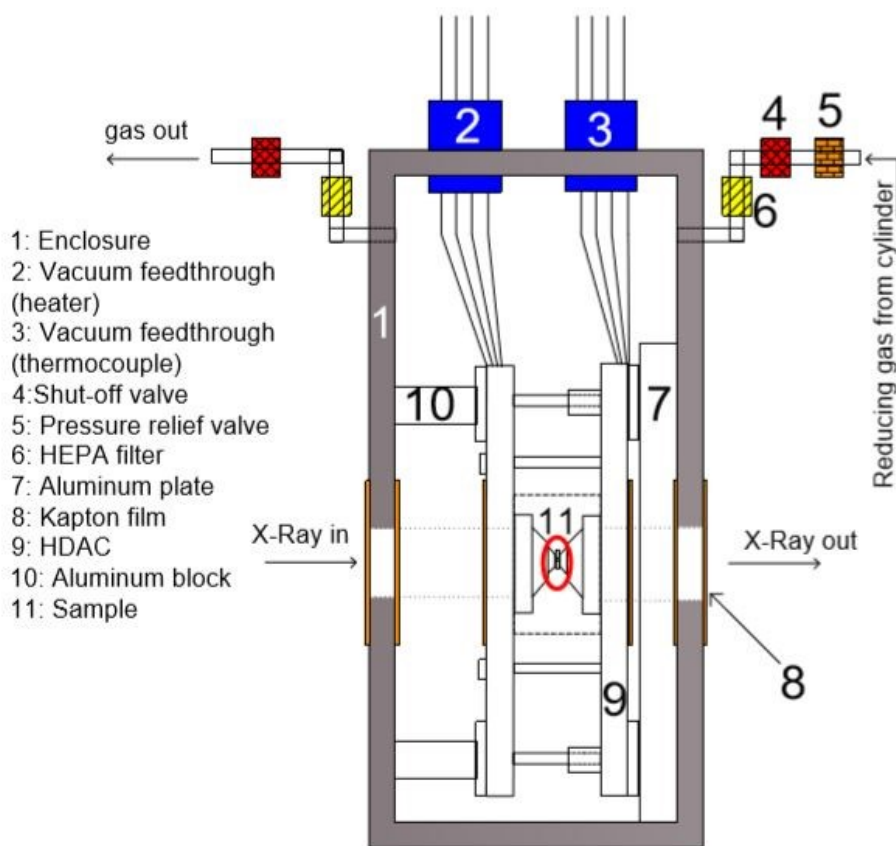
Fig. 3.2: Schematic diagram of the HDAC-enclosure assembly. The individual components are labeled and identified within the list shown.

of 99.99% at 0.1 μm, is placed after the shut-off valve on the inlet side of the gas line. Plastic ties

are used around each plumbing connection to ensure proper sealing. The outlet gas line also has

a HEPA filter and shut-off valve fitted to the gas line tubing, which, at the exit end, is dipped in

about 10 cm of water in a beaker used to monitor the flow of reducing gas through the cell and

enclosure.

Two 0.5-inch (1.27 cm) NPT threaded vacuum feedthroughs, one for the electrical

connections (Solid Sealing Technology) and the other for thermocouple connections (Omega),

are screwed and sealed into one end of the container of the enclosure (see Fig. 3.3 (a)). Each

feedthrough carries four wires, where the electrical feedthrough (Fig. 3.2, #2) has copper wires and the other has chromel-alumel wires for K-type thermocouples (Fig. 3.2, #3). Once the sample is loaded into the HDAC, it is positioned into a slotted aluminum plate that is screwed to
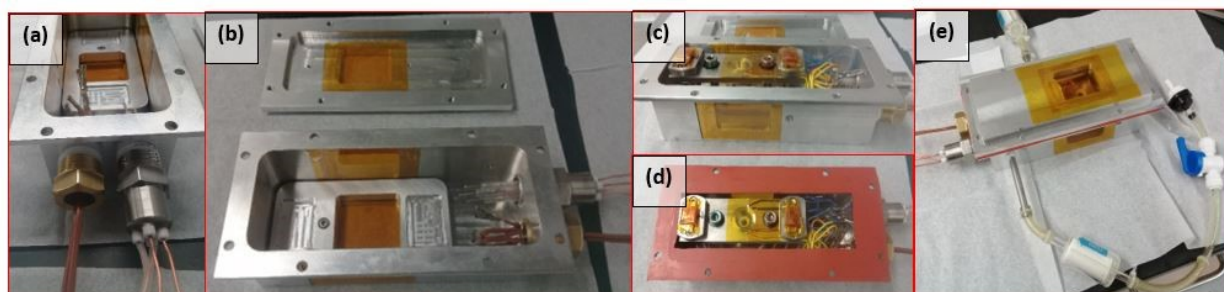

Fig. 3.3: Different stages of enclosure loading. (a) The feedthrough connectors attached to the container of the enclosure, (b) the container and lid portions, (c) the HDAC positioned into the container, (d) same as (c) but with the silicone gasket in place, and (e) the sealed enclosure fitted with gas lines, HEPA filters, pressure relief valve, and shut-off valves.

the bottom of the container, so that it is anchored in place upon final sealing of the enclosure (Fig. 3.3 (b)). In the exterior of the feedthrough connectors, the copper wires are joined with the wires from the HDAC heater using copper 2 pin male-female connectors whereas thermocouple wires are connected using K-type thermocouple 2 pin male-female connectors. In the interior of the container, the thermocouple wires are simply joined and twisted (to avoid introducing different material in line) before fixing them into position using heat shrinks. The same procedure is used for the heater wires. The slotted aluminum plate serves to not only anchor the HDAC but also helps in avoiding direct contact of the cell with the enclosure and in lessening direct heat transfer through metal parts. Two 1x1x2 cm aluminum blocks (Fig. 3.2, #10) are screwed into the inside of the lid, which press on the HDAC and anchor it within the enclosure during transport and experiment.

Experimental Procedure and Results

For the sample preparation, 0.148 gm of UO_3 powder was added slowly to 8 ml of 12.1 M HCl solution at 150 °C. The solution was stirred by slowly revolving the container in a circular fashion until a clear yellow solution was obtained. The resulting solution was evaporated slowly at 150 °C in approximately 2.5 hours to obtain a yellow $UO_2Cl_2 \cdot nH_2O$ residue. The residue was then dissolved in deionized water to obtain a clear yellow solution of approximately 0.05 M uranyl concentration. Then, 82.6 µl of 12.1 M HCl was added to lower the pH of the solution below 2. Finally, the chloride concentration was adjusted to 1 M by the addition of LiCl salt to the solution. This sample was loaded in the sample chamber of the HDAC. Fig. 3.4 shows the loaded sample as viewed along the loading axis of the HDAC. The loaded HDAC was
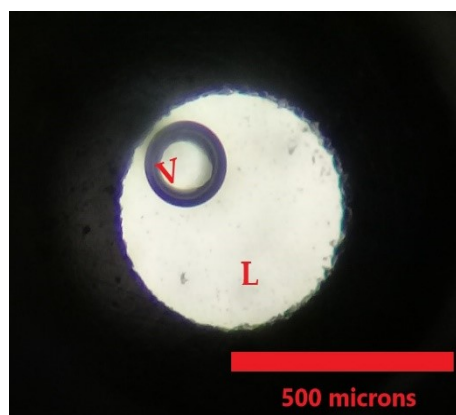
Fig. 3.4: Photomicrograph of the aqueous uranyl chloride sample in the HDAC showing the vapor (V) and liquid (L) portions.

anchored in the enclosure, which was subsequently sealed and fitted with gas lines. The enclosure was mounted on a motion stage at the APS 20-ID-C beamline as shown in Fig. 3.5: This configuration coincides with the loading axis of the HDAC being aligned with the incident x-ray beam. A 4-element Vortex detector was used for detection of the fluorescence signal. The

x-ray beam was focused using Kirkpatrick-Baez mirrors to approximately 150 μm. Detuning of the monochromator Si (111) crystals was set at 15 %. A 10.2 cm long N_2-gas filled ionization
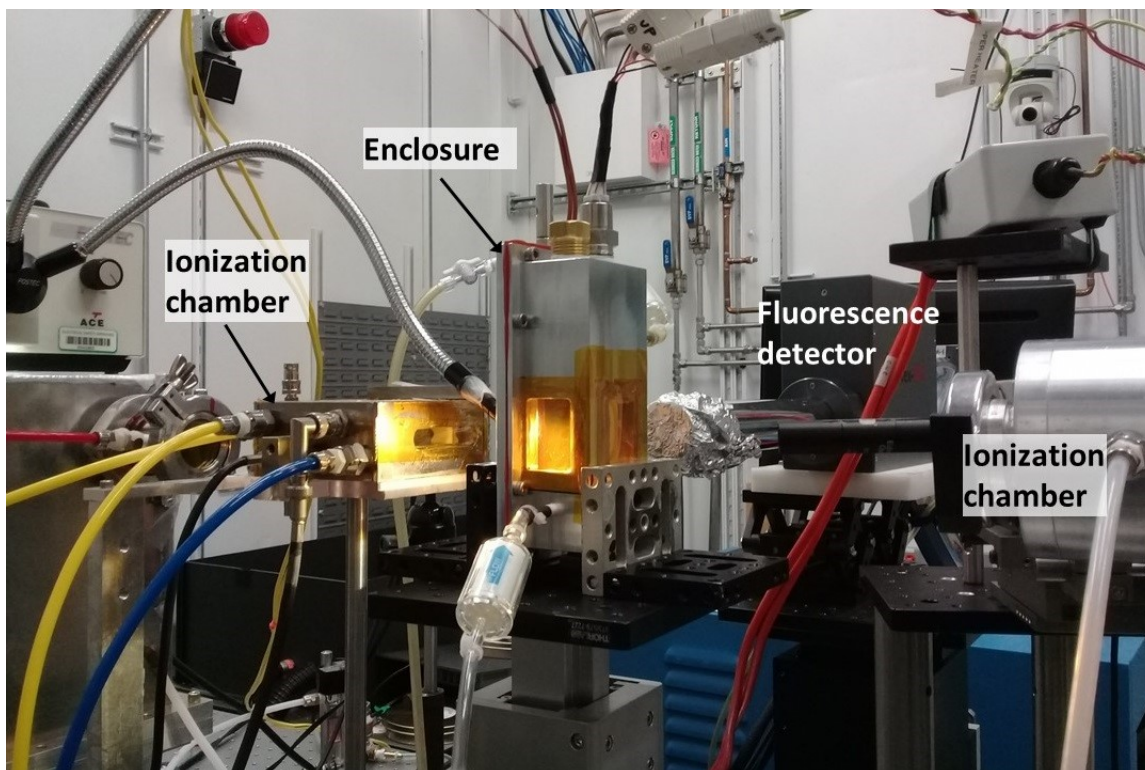
Fig. 3.5: Photograph showing the HDAC-enclosure assembly, containing the HDAC inside the enclosure, during experiments made at the 20-ID synchrotron beamline of the APS.

chamber was used to detect the incident x-ray beam. Sample pressure was estimated using the equation of state (EOS) of water [12]. The liquid-vapor homogenization temperature (T_H) was measured by microscopic observation of the sample and the pressure was determined at temperatures above T_H from the known isochores of the EOS of water. More detailed discussions of the procedures used to estimate pressures of aqueous samples using the HDAC can be found elsewhere [9].

The XAS data collected at beamline 20 ID-C of APS from the aqueous uranyl chloride sample at the U L_3 edge (17,166.3 eV) using my HDAC-enclosure assembly, from 25 °C and vapor pressure to 500 °C and approximately 350 MPa are shown in Fig. 3.6. Despite the use of the HDAC enclosure, the quality of data is comparable to that obtained from non-radioactive aqueous samples without an enclosure. XAS data collected from an aqueous uranyl sample in
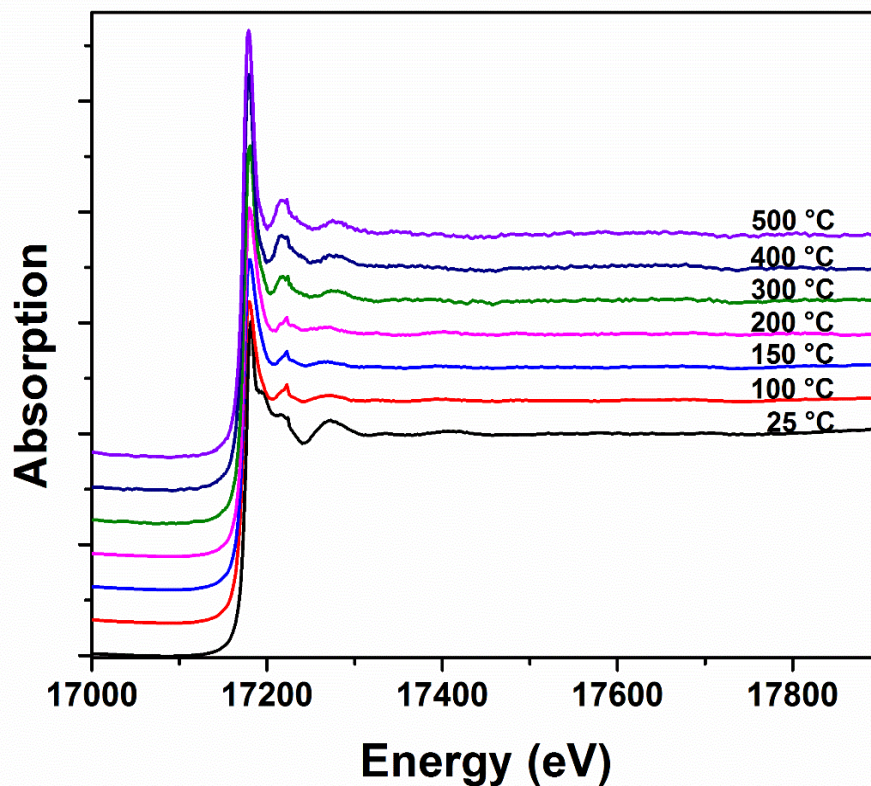

Fig. 3.6: XAS data collected from the aqueous uranyl chloride sample at the APS, at temperatures ranging from 25 to 500 °C, using our HDAC-enclosure assembly.

triflic acid solution up to 500 °C and approximately 270 MPa at the U L_3 edge at beamline 11-2 of SSRL using our HDAC-enclosure assembly exhibit very similar quality to that shown in Fig.

3.6. Real-time monitoring of the sample and T_H measurement using a video camera is an important experimental procedure in the use of the HDAC. The windows of the enclosure that are in line with the incident x-ray beam were designed to be sufficiently wide so as to enable viewing the sample off-beam axis using a video camera fitted with a long focal-length objective. The halogen light shown in Fig. 3.5 is used to illuminate the sample from the opposite side to the camera.

For XAS measurements made at high temperatures at the APS, the enclosure and the HDAC were continuously flushed with a 2% of H_2 and 98% of Ar gas mixture, and, for similar measurements made at SSRL, 99.9% pure Ar gas, at about 4 ltr/min flow rate to avoid oxidation of the diamond anvils, heater wires or any other cell parts. In addition to providing reducing environment conditions, the gas flow through the HDAC-enclosure assembly is also critical for providing reduced heat load conditions and ensuring safe temperature operating conditions of the exterior portion of the HDAC and of the enclosure.

The change in temperature of the enclosure upon heating the sample was measured and recorded in a separate benchtop test, using the same 4 l/min gas flow rate and identical conditions for the experiment, to assess the integrity and safety of the components used in the HDAC-enclosure assembly. The temperature measurement was made using a type-K chromel-alumel thermocouple attached directly to the outside of the enclosure at a point of closest proximity to the HDAC. The plot of temperature of the enclosure and of the sample in the HDAC vs. time is shown in Fig. 3.7. The maximum temperature of the enclosure reached 79 °C with a corresponding maximum temperature of the sample in the HDAC at 505 °C. The temperature of the sample was maintained at 505 °C for approximately 3.5 hours to assess the equilibrium temperature of the enclosure. As can be seen in the inset of Fig. 3.7, it takes about 20

minutes for the temperature of the enclosure to equilibrate to 79 °C with the sample at 505 °C.

The results of this benchtop experiment reveal that the temperature of the enclosure remains well below the temperature of the sample and sufficiently low to ensure safe operation of the HDAC-enclosure assembly. An additional benchtop test was made to assess the integrity of the Kapton windows by closing the reducing gas-outlet and allowing the gas to build up in the enclosure until the inline pressure reached 15 psi. The windows retained their integrity to this pressure, which is 10 times the inline pressure used during experiments, without any traceable damage.
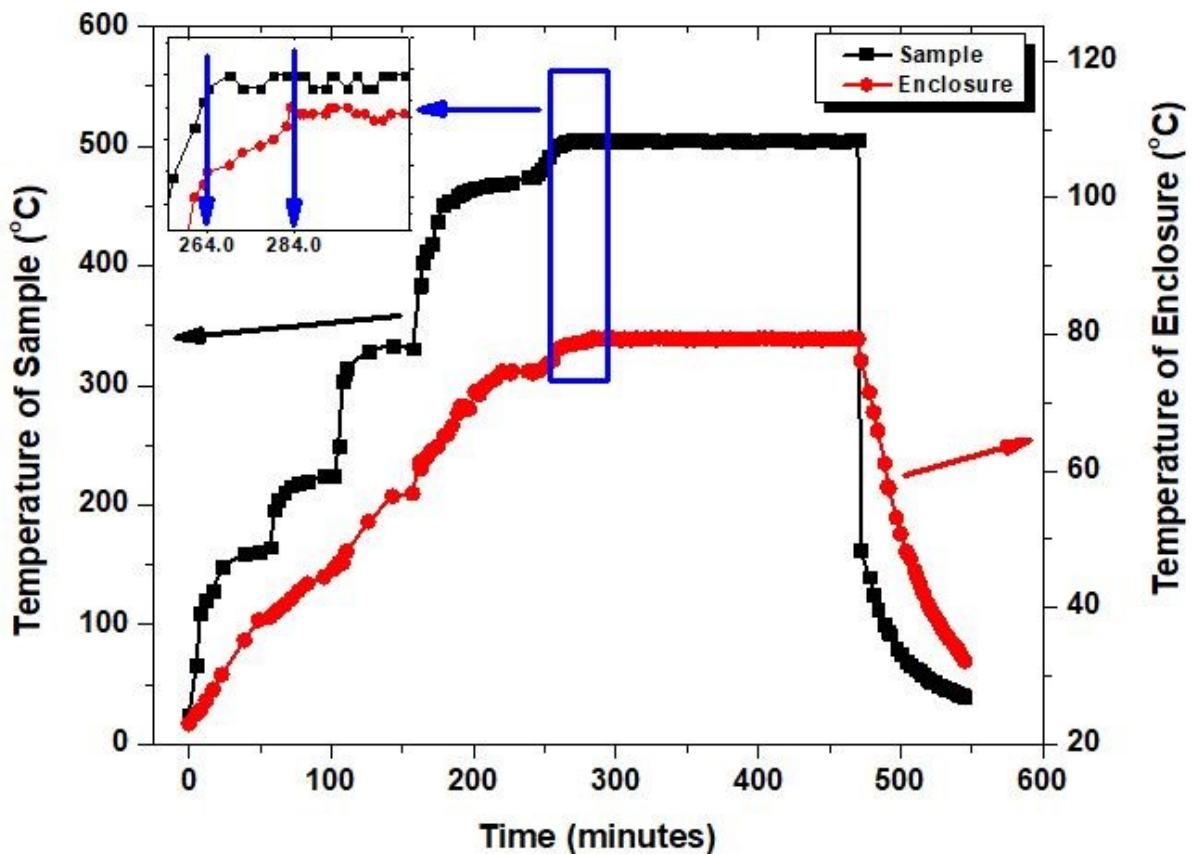

Fig. 3.7: Temperature of the sample in the HDAC and of the enclosure with respect to time under experimental conditions described in the text.

Discussion

The requirements for an enclosure for the HDAC containing aqueous radioactive solutions measured at synchrotron facilities to high P-T conditions are: 1) to have the ability to maintain integrity and full containment fulfilling the safety requirements of the synchrotron facilities, 2) to allow for transmission of incident x-ray beam and for measurement of fluorescence x-ray signal from actinide-bearing aqueous solutions, 3) to enable sufficient cooling of the external portions of the HDAC and enclosure so as to ensure safe operating conditions, 4) to maintain both electrical and thermocouple connections from the controller to the HDAC, and 5) to enable real-time visual monitoring of the sample via a suitable video-microscope setup. The enclosure must satisfy these requirements to at least 500 °C measurement temperature and under nominal gas pressures. My tests made at both APS and SSRL as well as the benchtop test in the laboratory show that depleted uranium aqueous samples can be successfully measured at up to 500 °C and 0.5 GPa pressure using my HDAC-enclosure assembly, within the conditions outlined above. In order to extend the use of this enclosure for the HDAC to measure transuranic elements in aqueous solutions, an improvement on the second layer of the containment may be needed, due to the increased safety requirements for such samples. The second layer partially consists of Kapton tape affixed to a cylindrical steel frame collar surrounding the sample chamber of the HDAC. For use with transuranic samples, this collar needs to be completely sealed against the platens, which can be accomplished by using suitable O-rings on the edges of the collar. Moreover, although my initial tests of the HDAC-enclosure assembly were made by measurements of samples to relatively high pressures, measurements can also be made at low pressure conditions in order to create a sample environment more reflective of conditions

anticipated at geological repositories and nuclear reactors. This can easily be accomplished by increasing the sample vapor/liquid ratio upon loading the HDAC. Finally, it is important to note that in addition to XAS studies, my enclosure has the potential to be used for a broader variety of synchrotron measurements of aqueous and non-aqueous (e.g., CO_2, SO_3, etc.) fluid radioactive samples contained in the HDAC, including x-ray diffraction (XRD), x-ray fluorescence (XRF), and small (SAXS) and wide angle x-ray scattering (WAXS).

Acknowledgements

References

[1] M. J. Apted and J. Ahn, "Geological repository systems for safe disposal of spent nuclear fuels and radioactive waste," Woodhead Publishing, 2017.

[2] K. A. Rogers, "Fire in the hole: A review of national spent nuclear fuel disposal policy," *Progress in Nuclear Energy*, vol. 51, no. 2, pp. 281–289, Mar. 2009.

[3] J. Birkholzer, J. Houseworth, and C.-F. Tsang, "Geologic disposal of high-level radioactive waste: status, key issues, and trends," *Annual Review of Environment and Resources*, vol. 37, no. 1, pp. 79–106, 2012.

[4] J.-S. Kim, S.-K. Kwon, M. Sanchez, and G.-C. Cho, "Geological storage of high-level nuclear waste," *KSCE J Civ Eng*, vol. 15, no. 4, pp. 721–737, Apr. 2011.

[5] IAEA, "Accident tolerant fuel concepts for light water reactors," 2016.

[6] S. Bragg-Sitton, "Development of advanced accident-tolerant fuels for commercial LWRs," *Nuclear News*, pp. 83–91, Mar-2014.

[7] F. Nagase, K. Sakamoto, and S. Yamashita, "Performance degradation of candidate accident-tolerant cladding under corrosive environment," *Corrosion Reviews*, vol. 35, no. 3, pp. 129–140, 2017.

[8] A. J. Anderson and R. A. Mayanovic, "X-ray absorption spectroscopy studies in supercritical aqueous solutions," *High Pressure Research*, vol. 36, no. 3, pp. 458–470, Jul. 2016.

[9] W. A. Bassett, A. H. Shen, M. Bucknum, and I. Chou, "A new diamond anvil cell for hydrothermal studies to 2.5 GPa and from −190 to 1200 °C," *Review of Scientific Instruments*, vol. 64, no. 8, pp. 2340–2345, Aug. 1993.

[10] H. Yan, R. A. Mayanovic, A. J. Anderson, and P. R. Meredith, "An in situ X-ray spectroscopic study of Mo6+ speciation in supercritical aqueous solutions," *Nuclear Instruments and Methods in Physics Research Section A: Accelerators, Spectrometers, Detectors and Associated Equipment*, vol. 649, no. 1, pp. 207–209, Sep. 2011.

[11] A. J. Anderson, H. Yan, R. A. Mayanovic, G. Solferino, and C. J. Benmore, "High-energy X-ray diffraction of a hydrous silicate liquid under conditions of high pressure and temperature in a modified hydrothermal diamond anvil cell," *High Pressure Research*, vol. 34, no. 1, pp. 100–109, Jan. 2014.

[12] W. Wagner and A. Pruß, "The IAPWS Formulation 1995 for the thermodynamic properties of ordinary water substance for general and scientific use," *Journal of Physical and Chemical Reference Data*, vol. 31, no. 2, pp. 387–535, Jun. 2002.

SUMMARY

There is presently a lack of high pressure-temperature (P-T) data on the speciation of aqueous uranyl chloride complexes covering a wide range of chloride and uranyl concentrations. I have performed in-situ high P-T experiments using a hydrothermal diamond anvil cell and Raman spectroscopy on aqueous uranyl chloride solutions having chloride concentrations varying between 0.12 to 3 M. Careful processing and analysis of the Raman spectra has led generating unprecedented knowledge of the types and amounts of different uranyl-chloride species occurring at different temperatures form 25 to 500°C and pressures ranging from vapor to 500 MPa. A clear evolution and a gradual red-shift of the overall Raman stretching mode vibration band of the uranyl-chloride aqueous complexes occurs with increase in temperature and/or chloride concentration, which is attributed to the changing speciation with the change in temperature and Cl concentration parameters. The overall Raman stretching mode vibration band was fit using a maximum of 4 peaks, corresponding to UO_2^{2+}, UO_2Cl^+, $UO_2Cl_2^0$ and $UO_2Cl_3^-$. The peak position and FWHM of each species were determined at each temperature point and for each of the aqueous solutions of the study. The peak positions for each of the species show a consistent and gradual blue-shift of the vibration maxima, which is consistent with the behavior of the uranyl chloride complexes and can be explained as due to the enhancement in thermal effects at higher temperatures. From the corresponding areas under the peaks for each species in the fitted Raman spectra, the percentage contributions of each specie towards the overall speciation were calculated and plotted for different temperatures of same samples and for constant temperatures with varying chloride concentrations (Chapter 1: Fig. 2.5 and 2.6). These plots show gradual and systematic increase in stability of complexes with increasing number of

chloride ligands up to 2. At higher temperatures the neutral specie $UO_2Cl_2^0$ dominates most of the chloride concentration range studied here. The results of this study are generally consistent with the high temperature (to 250°C) study made using UV-Vis spectroscopy method by Migdisov *et al.* [9]. However, the results from my study contradict those obtained from a previous Raman study by Dargent *et al.* [10].

To compliment the results obtained from Raman study, I also worked on the development of an XAS study of the same aqueous solutions. The stringent requirements of DOE synchrotron facilities for the containment of such samples required the design and test of a radiological containment system (enclosure) described in Chapter 2 of this thesis. The enclosure was finalized after several iterations and testing at synchrotron beamlines at the APS and SSRL. This enclosure system should prove valuable for the researchers working on radioactive aqueous samples for high pressure high temperature experiments in the future. During and after the successful implementation and approval of the enclosure at both APS and SSRL, some of the samples on which Raman was performed were measured for XAS and data were collected. For the purpose of this thesis, the design and implementation of the enclosure for the XAS measurements of radioactive sample in hydrothermal conditions was presented and a set of data measured at temperatures ranging from 25 to 500°C, and pressures ranging from vapor to ??, was obtained. Thus, this demonstrates a successful implementation of the containment enclosure system for synchrotron XAS studies or aqueous actinide systems.

In the future, this project will be extended to study the Raman spectra of samples with even higher chloride concentration to obtain a comprehensive uranyl chloride complexing speciation under hydrothermal conditions. In addition, the XAS studies will also be executed on more samples with varying chloride concentrations under high P-T conditions and the results

will be compared with the speciation distributions obtained from this Raman study and with the results of other studies.

REFERENCES

[1] X. Liu, J. Cheng, M. He, X. Lu, and R. Wang, "Acidity constants and redox potentials of uranyl ions in hydrothermal solutions," *Physical Chemistry Chemical Physics*, vol. 18, no. 37, pp. 26040–26048, 2016.

[2] M. J. Apted and J. Ahn, "Geological repository systems for safe disposal of spent nuclear fuels and radioactive waste," Woodhead Publishing, 2017.

[3] K. A. Rogers, "Fire in the hole: A review of national spent nuclear fuel disposal policy," *Progress in Nuclear Energy*, vol. 51, no. 2, pp. 281–289, Mar. 2009.

[4] J. Birkholzer, J. Houseworth, and C.-F. Tsang, "Geologic disposal of high-level radioactive waste: status, key issues, and trends," *Annual Review of Environment and Resources*, vol. 37, no. 1, pp. 79–106, Nov. 2012.

[5] J.-S. Kim, S.-K. Kwon, M. Sanchez, and G.-C. Cho, "Geological storage of high-level nuclear waste," *KSCE Journal of Civil Engineering*, vol. 15, no. 4, pp. 721–737, Apr. 2011.

[6] S. Bragg-Sitton, "Development of advanced accident- tolerant fuels for commercial LWRs," *Nuclear News*, pp. 83–91, Mar-2014.

[7] IAEA, "IAEA Report-Accident tolerant fuels." 2016.

[8] E. Tertre, "Europium retention onto clay minerals from 25 to 150°C: Experimental measurements, spectroscopic features and sorption modelling," *Geochimica et Cosmochimica Acta*, vol. 70, no. 18, pp. 4563–4578, Sep. 2006.

[9] A. A. Migdisov, H. Boukhalfa, A. Timofeev, W. Runde, R. Roback, and A. E. Williams-Jones, "A spectroscopic study of uranyl speciation in chloride-bearing solutions at temperatures up to 250 °C," *Geochimica et Cosmochimica Acta*, vol. 222, pp. 130–145, Feb. 2018.

[10] M. Dargent, J. Dubessy, L. Truche, E. F. Bazarkina, C. Nguyen-Trung, and P. Robert, "Experimental study of uranyl(VI) chloride complex formation in acidic LiCl aqueous solutions under hydrothermal conditions (T = 21 C–350 °C, Psat) using Raman spectroscopy," *European Journal of Mineralogy*, vol. 25, no. 5, pp. 765–775, Oct. 2013.

[11] Oreskes and Einaudi, "Origin of hydrothermal fluids at Olympic Dam; preliminary results from fluid inclusions and stable isotopes," *Economic Geology, GeoScienceWorld*, 1992.

[12] A. Richard, C. Rozsypal, J. Mercadier, D. A. Banks, M. Cuney, M. Boiron, and M. Cathelineau, "Giant uranium deposits formed from exceptionally uranium-rich acidic brines," *Nature Geoscience*, vol. 5, p. 142, Dec. 2011.

[13] M. Cuney, "The extreme diversity of uranium deposits," *SpringerLink,* 2009. [Online]. Available: https://link.springer.com/article/10.1007%2Fs00126-008-0223-1. [Accessed: 17-Mar-2019].

[14] Derome, "Mixing of sodic and calcic brines and uranium deposition at McArthur River, Saskatchewan, Canada: A Raman and laser-induced breakdown spectroscopic study of fluid inclusions," *Economic Geology, GeoScienceWorld,"* 2005. [Online]. Available: https://pubs.geoscienceworld.org/segweb/economicgeology/article-abstract/100/8/1529/127679. [Accessed: 17-Mar-2019].

[15] L. Kish and M. Cuney, "Uraninite-albite veins from the Mistamisk Valley of the Labrador Trough, Quebec," *Mineralogical Magazine*, vol. 44, no. 336, pp. 471–483, Dec. 1981.

[16] M. Z. Min, X. Z. Luo, and S. L. Mao, "The Saqisan Mine — a paleokarst uranium deposit, South China," *ScienceDirect,* 2002. [Online]. Available: https://www.sciencedirect.com/science/article/pii/S016913680000010X. [Accessed: 17-Mar-2019].

[17] K. J. Wenrich and S. R. Titley, "Uranium exploration for northern Arizona (USA) breccia pipes in the 21st century and consideration of genetic models," p. 16, 2009.

[18] R. Guillaumont, T. Fanghanel, J. Fuger, and I. Grenthe, "Guillaumont: Update on the chemical thermodynamics," *Google Scholar,* 2003. [Online]. Available: http://www.wipp.energy.gov/library/cra/2009_cra/references/Others/Guillaumont_et_al_2003_Update_on_Chemical_Thermodynamics.pdf. [Accessed: 17-Mar-2019].

[19] A. A. Migdisov, "Hydrothermal transport, deposition, and fractionation of the REE: Experimental data and thermodynamic calculations." *ScienceDirect*, 2016.

[20] S. Ahrland, "On the Complex Chemistry of the Uranyl Ion," *Acta chemica scandinavica*, 1951.

[21] Choppin and Du, "*f*-Element Complexation in Brine Solutions," *Radiochimica Acta,* 1992.

[22] Davies and Monk, "Spectrophotometric studies of electrolytic dissociation. Part 4.—Some uranyl salts in water," *Transactions of the Faraday Society (RSC Publishing),* 1957.

[23] Soderholm, "Structural correspondence between uranyl chloride complexes in solution and their stability constants," *The Journal of Physical Chemistry A (ACS Publications),* 2011. [Online]. Available: https://pubs.acs.org/doi/10.1021/jp111551t. [Accessed: 17-Mar-2019].

[24] C. Hennig, J. Tutschku, A. Rossberg, and A. C. Scheinost, "Comparative EXAFS investigation of Uranium (VI) and -(IV) aquo chloro complexes in solution using a newly developed spectroelectrochemical cell," *Inorganic Chemistry (ACS Publications),* 2005.

[Online]. Available: https://pubs.acs.org/doi/abs/10.1021/ic048422n. [Accessed: 17-Mar-2019].

[25] A. J. Anderson, H. Yan, R. A. Mayanovic, G. Solferino, and C. J. Benmore, "High-energy X-ray diffraction of a hydrous silicate liquid under conditions of high pressure and temperature in a modified hydrothermal diamond anvil cell," *High Pressure Research*, Vol 34, No 1," 2014.